Water solubilization capacity of mixed reverse micelles: Effect of surfactant component, the nature of the oil, and electrolyte concentration

Bidyut K. Paul *, Rajib K. Mitra

Geological Studies Unit, Indian Statistical Institute, 203 B.T. Road, Kolkata 700108, India

Received 29 November 2004; accepted 18 February 2005

Available online 19 April 2005

Abstract

Solubilization of water in mixed reverse micellar systems with anionic surfactant (AOT) and nonionic surfactants (Brijs, Spans, Tweens, Igepal CO 520), cationic surfactant (DDAB)–nonionic surfactants (Brijs, Spans, Igepal CO 520), and nonionic (Igepal CO 520)–nonionics (Brijs, Spans) in oils of different chemical structures and physical properties (isopropyl myristate, isobutyl benzene, cyclohexane) has been studied at 303 K. The enhancement in water solubilization has been evidenced in these systems with some exceptions. The maximum water solubilization capacity ($\omega_{0,\max}$) in mixed reverse micellar systems occurred at a certain mole fraction of a nonionic surfactant, which is indicated as $X_{\text{nonionic},\max}$. The addition of electrolyte (NaCl or NaBr) in these systems tends to enhance their solubilization capacities further both at a fixed composition of nonionic (X_{nonionic}; 0.1) and at $X_{\text{nonionic},\max}$ at 303 K. The maximum in solubilization capacity of electrolyte ($\omega_{\max}$) was obtained at an optimal electrolyte concentration (designated as $[\text{NaCl}]_{\max}$ or $[\text{NaBr}]_{\max}$). All these parameters, $\omega_{0,\max}$ vis-à-vis $X_{\text{nonionic},\max}$ and $\omega_{\max}$ vis-à-vis $[\text{NaCl}]_{\max}$, have been found to be dependent on the surfactant component (content, EO chains, and configuration of the polar head group, and the hydrocarbon moiety of the nonionic surfactants) and type of oils. The conductance behavior of these systems has also been investigated, focusing on the influences of water content (ω), content of nonionics (X_{nonionic}), concentration of electrolyte ([NaCl] or [NaBr]), and oil. Percolation of conductance has been observed in some of these systems and explained by considering the influences of the variables on the rigidity of the oil/water interface and attractive interactions of the surfactant aggregates. Percolation zones have been depicted in the solubilization capacity vs X_{nonionic} or [electrolyte] curves in order to correlate with maximum in water or electrolyte solubilization capacity. The overall results, obtained in these studies, have been interpreted in terms of the model proposed by Shah and co-workers (Langmuir 3 (1987) 1086; J. Colloid Interface Sci. 120 (1987) 320 and 330) for the solubility of water in water-in-oil microemulsions, as their model proposed that the two main effects that determine the solubility of these systems are curvature of the surfactant film separating the oil and water and interactions between water droplets.

Keywords: Solubilization; Mixed reverse micelles; AOT; DDAB; Brijs; Isopropyl myristate; Percolation of conductance

1. Introduction

Reverse micellar systems have attracted the attention of research workers from various fields of science and technology owing to their unique ability to solubilize water in organic solvents in the presence of surfactants [1–14]. The water molecules solubilized in the interior of the water pool have properties different from those of bulk water. This makes reverse micellar systems potentially useful in industry and technology [1–8] and biologically important systems [9–14]. Solubilization of water in reverse micellar systems has been found to be dependent on various factors such as the rigidity of the interfacial film, which in turn depends upon the size of the polar head group and hydrocarbon moiety of the surfactant, the composition, the type of oils, the presence of electrolyte, the na-

ture and valence of the counterion, the temperature, etc. [1,15–17].

Kon-No et al. [16,18,19] first reported on the solubilization behavior of reverse micellar systems using surfactants such as dodecylammonium carboxylate, butyl dodecyldimethyl ammonium bromide, polyoxyethylene nonyl phenyl ether, and sodium bis(2-ethylhexyl) sulfosuccinate (AOT) in organic solvents at different temperatures in the absence and in the presence of electrolytes of different charge types. They also investigated the solubilization behavior of AOT-based reverse micellar systems in paraffin and naphthenic and aromatic solvents [20]. Kawai et al. [21,22] reported the solubilization behavior of anionic, AOT- and cationic, butyldodecyl dimethylammonium bromide (BDDAB)-based reverse micellar systems in different oils (cyclohexane, heptane, isooctane, dodecane, toluene, and chlorobenzene). Recently they [23] investigated the solubilization behavior and state of water in the water pool of an AOT/isooctane reverse micellar system in the presence of salts of different charge types. The results were interpreted in terms of salting-in and salting-out phenomena and counteracting effects of attractive intermicellar interaction and interfacial bending stress.

Bansal et al. [24] studied the solubilization capacity of reverse micelles formed with fatty acid soaps and alcohols as a function of alkyl chain of oils, soap, and alcohol and found that the maximum solubilization was observed when chain length compatibility was reached.

Solubilization of water in AOT-based reverse micellar systems in various hydrocarbon oils of different chain length both in the absence and in the presence of additives (a second surfactant, electrolyte, and alcohols) has been carried out by Shah and co-workers [25–28]. They studied the effect of chain length of oil and nature of additives on the solubilization behavior of such systems. A comprehensive model of the mechanism that governs the solubilization process in reverse micellar/water-in-oil microemulsion systems was proposed by them. Zana and co-workers [29,30] made a systematic investigation to determine the water solubility in reverse micelles made up of cationic surfactants in aromatic solvents, as a function of the surfactant chain length, the size of the head group, and the nature of the counterion for a homologous series of surfactants. The effect of oil was also investigated by considering aromatic solvents of different physical properties. This study was aimed at checking the prediction of the model relating the change in water solubility of water to parameters such as the surfactant chain length and head group size of the cationic surfactants. Derouiche and Tondre [31] studied the solubilization of water in AOT/decane or dodecane reverse micellar systems in the presence of different monovalent and divalent salts and correlated the water/electrolyte maxima with a dramatic change in conductivity. They explained their results on the basis of a possible existence of the Debye screening length. Later [32], they examined the rate of water uptake by AOT/decane reverse micellar systems in the absence and presence of different additives (NaCl, polyoxyethylene glycols (POEG), and *n*-alkanols) using the stopped-flow technique with turbidity detection and conductivity measurements, and correlated the rate constant of the solubilization process with percolating and nonpercolating systems. The solubility of water in w/o microemulsions stabilized by cetyltrimethyl ammonium (CTA) has been investigated as a function of the nature of the surfactant counterion (bromide, CTAB/chloride, CTAC), the composition of the oil (chloroform and chloroform/heptane mixtures), the salting of the droplets, and the nature of the salt employed to modify it [33]. Strong alterations of the solubility of water were found to occur upon mixing of the surfactants. The results of all these studies cited above were explained in terms of the model proposed by Shah et al. [25–27].

Anionic surfactant, AOT, is the most widely studied surfactant in the field of solubilization in reverse micelles owing to its ability to form reverse micelles in hydrocarbon oils at different concentrations. On the other hand, cationic surfactant, DDAB [34–37], and nonionic surfactants Igepal [38,39] have also been reported to form reverse micelles in hydrocarbon oils. All of these investigations cited involve single-surfactant reverse micelles. Such studies in reverse micelles consisting of more than one surfactant are rarely reported. Formulation of an alcohol-free microemulsion using pharmaceutically acceptable high-molecular-weight surfactants (AOT and Span-20) in mixed proportions, and the effects of hydrocarbon chain length (C_7–C_{16}) and electrolytes on water solubilization in these mixed microemulsions have been reported by Johnson and Shah [40,41]. Huibers and Shah further reported [42] the solubilization behavior of nonionic–nonionic mixed surfactant systems using the series of nonylphenyl ethoxylates (Igepal CO family of surfactants) in cyclohexane. Two different approaches to surfactant selection (from the viewpoint of their HLB numbers vis-à-vis high solubility in oil and water) were made in order to achieve a high level of water solubilization in w/o microemulsion formulations. Ludensten et al. [43] reported an enhancement of water solubilization in AOT–alkyl phenyl ethoxylate mixed surfactant reverse micellar systems in aromatic oils. Seedher and Manik [44] observed synergism in solubilization capacity for mixed cationic (CTAB, CPC)–anionic (AOT) or nonionic (Brij-30, TX-100) surfactant systems in hydrocarbon oils (cyclohexane, hexane, octane, benzene). They reported that solubilization increased with decrease in polarity and increase in chain length of solvent. Liu et al. [45] observed a maximum solubilization capacity of water in the presence of a certain concentration of NaCl (C_{max}) for mixed reverse micellar systems formed with AOT and nonionic surfactants (Brijs) in hydrocarbon oils (cyclohexane, hexane, heptane, octane, and isooctane). C_{max} has been reported to depend upon the nature of the added nonionic surfactant and the molar volume of oil. Li et al. [46] reported that the presence of optimal content of bis-(2-ethylhexyl)phosphoric acid (HDEHP) remarkably enhanced the water solubilization capacity of the sodium bis-

(2-ethylhexyl) phosphate (NaDEHP)/heptane system, while it decreased the solubilization capacity of AOT/heptane system. The addition of a low concentration of NaCl in AOT microemulsions enhanced its solubilization capacity. The conductance behavior of the AOT system has been investigated, focusing on the influence of the HDEHP content, NaCl concentration, and temperature. Eastoe et al. [47] investigated solubilization of water in mixed cationic (DDAB)–cationic (DTAB)/ or nonionic ($C_{12}E_5$)/ or anionic (SDS) systems stabilized in heptane. They observed enhancement in solubilization capacity for both DDAB–DTAB and DDAB–$C_{12}E_5$ blends, whereas solubilization capacity has been reported to be decreased for DDAB–SDS blends. They obtained a sudden increase in conductance for DDAB/DTAB mixed systems. On the other hand, no such observation was noted for the other two systems. The structural features of these mixed reverse micellar systems were explored with the help of small angle neutron scattering (SANS) and other techniques. They showed that changes in microemulsion phase behavior and properties are a direct consequence of preferred film curvature, which can be varied by surfactant mixing in the interface. Very recently, they [48] investigated the electrical conductivity of D_2O-in-*n*-heptane (or -in-*p*-xylene) microemulsions stabilized by a mixture of the cationic surfactant di-*n*-didodecyldimethylammonium bromide, DDAB, and either the C_iE_j nonionic surfactants or the polymeric nonionic surfactants of the type PEO–PPO–PEO, Pluronic, as a function of D_2O content and surfactant mixture composition. They interpreted the results on the basis of the charge fluctuation model (CFM).

Till now, most of the studies regarding the solubilization phenomenon in reverse micellar systems stabilized by both single and mixed surfactant systems have been carried out using hydrocarbon oil as solvent. The type of surfactants and their chemical structures as well as oils played a significant role in the solubilization process. Such studies in a polar oil like isopropyl myristate (IPM), which possesses different physical properties and structure as compared to the hydrocarbon oils, are scarce. In addition, IPM finds application in biologically relevant microemulsion systems [49–51]. The microstructural aspects of these mixed reverse micellar systems using this type of oil has not been explored. In continuation of our previous studies [52–56] on the phase behavior as well as the conductance behavior of mixed surfactant microemulsion/reverse micellar systems stabilized in various types of oils, a systematic investigation of the solubilization behavior of mixed surfactant reverse micellar systems using anionic (AOT)–nonionic(s) (Brijs, Spans, Tweens, Igepal), cationic (DDAB)–nonionic(s) (Brijs, Spans), and nonionic (Igepal)–nonionic(s) (Brijs, Spans) in IPM oil both in absence and presence of electrolytes has been carried out. These results have been compared with other solvents with different physical properties and chemical structures [alicyclic hydrocarbon oil (Cy), aromatic oil (IBB), and a straight-chain hydrocarbon oil (Dc)]. An attempt has been taken to explain all these results on the basis of the model developed by Shah and co-workers [25–27] taking into account the role of nonionic surfactant (its content, configuration of polar head group and hydrophobic moiety), oils (of different physical properties and structure), concentration of the electrolyte, and water content. In this report, the appearance of maximum in solubilization capacity has been correlated with the microstructural variation due to the occurrence of percolation of conductance both in absence and presence of the electrolytes. The conductance behaviors have been interpreted by considering the influence of these variables on the rigidity and attractive interaction of the surfactant aggregates.

2. Materials and methods

The following surfactants were used without further purification, sodium bis(2-ethylhexyl) sulfosuccinate (AOT, 99%), polyoxyethylene(20) sorbitan monolaurate (Tween-20), and polyoxyethylene(20) sorbitan monopalmitate (Tween-40) were purchased from Sigma, USA. Nonylphenyl ethoxylate (Igepal CO 520) was a product of Aldrich, USA. Polyoxyethylene(4) lauryl ether (Brij-30), polyoxyethylene(23) lauryl ether (Brij-35), polyoxyethylene(2) cetyl ether (Brij-52), polyoxyethylene(10) cetyl ether (Brij-56), polyoxyethylene(20) cetyl ether (Brij-58), polyoxyethylene(10) stearyl ether (Brij-76), sorbitan monolaurate (Span-20), sorbitan monopalmitate (Span-40), sorbitan monostearate (Span-60), sorbitan monooleate (Span-80), and didodecyldimethylammonium bromide (DDAB) were products of Fluka (Switzerland). Chemical structures of some of the surfactants are presented in Scheme 1 (see Supplementary Material). Cyclohexane (Cy), isobutylbenzene (IBB), 2-ethylhexanol, NaBr, and NaCl were AR and extrapure grade products of SRL, India. Isopropyl myristate (IPM) was a product of Fluka (Switzerland) and its density and refractive index agreed well with the literature. Decane (Dc) and Eugenol (Eu) were products of Fluka (Switzerland) and Loba Chemicals (India), respectively, and were used as received. Sudan IV and Eosin Blue were AR grade products of SRL, India.

Double-distilled water with conductance less than 3 μS cm^{-1} was used.

Stock solutions of all the surfactants mentioned above were made in different oils, and mixed anionic (AOT), cationic (DDAB), and nonionic (Igepal CO 520) in different proportions with nonionic surfactants to vary X_{nonionic}, where X denotes the mole fraction of nonionic surfactant in total surfactant,

$$X_{\text{nonionic}} = \frac{[\text{nonionic}]}{[\text{nonionic}] + [\text{ionic}]}.$$

The surfactant solution was fixed at a concentration of 0.1 mol dm^{-3} if not mentioned otherwise. These solutions were taken in sealed test tubes, equilibrated in a thermostatic water bath at 303 K, and titrated with water [or aqueous

NaCl (NaBr) at different concentrations] using a microsyringe of varying capacity with constant stirring in a vortex shaker. The onset of permanent turbidity at each composition of surfactant mixture in oil denotes maximum solubilization of water or aqueous NaCl (NaBr) at the end point of titration. All the experiments were repeated two or three times and mean results were taken. In order to check the behavior of the phase separation at the saturation of solubilization (i.e., at equilibrium), we used two dyes: Eosin Blue (EB), which is selectively soluble in water, and Sudan IV, which is selectively soluble in oils [25,29,30,45]. These systems were allowed at least 1 h time at 303 K in order to ensure complete phase separation. The different phases, as well as Winsor types, have been identified in accordance with the different colors developed due to the solubilization of these two dyes (of different characteristics) in these mixed systems. The results of these experiments have been dealt in the subsequent section.

Conductivity measurements were made using an automatic temperature-compensated conductivity meter, Thermo Orion, USA (Model 145A plus), at 303 K, with cell constant 1.0 cm^{-1}. The uncertainty in measurement was not more than ±1%.

3. Results and discussion

3.1. Solubilization of water in mixed reverse micelles in oils (IPM, Cy, IBB)

Water solubilization capacity of anionic (AOT)–nonionics (Brijs, Tweens, Spans and Igepal), cationic (DDAB)–nonionics (Brijs, Spans) and nonionic (Igepal)–nonionic (Brijs, Spans) mixed reverse micelles in three different types of oils (IPM, IBB and Cy with molar volumes of 317, 157, and 108 $cm^3\ mol^{-1}$, respectively) and water are presented in Figs. 1–3 and Table 1.

3.1.1. Effect of total surfactant concentration on solubilization of water in IPM, Cy, IBB

Fig. 1 depicts the solubilization behavior of AOT/Brij-56/oil (IPM, IBB, and Cy) reverse micellar systems at three different surfactant concentrations, viz. 0.1, 0.175, and 0.25 mol dm^{-3} at 303 K. The maximum amount of water solubilized ($\omega_{0,max}$) in AOT/Brij-56 mixed systems has been obtained at $X_{Brij\text{-}56,max} = 0.1$ (where $X_{Brij\text{-}56,max}$ is the mole fraction of Brij-56, at which maximum solubilization occurred) for all three oils. The total surfactant concentration, [S_T], has a small effect on $\omega_{0,max}$ for the AOT/Brij-56/IPM (30.0–30.5) and AOT/Brij-56/Cy (63.0–68.0) systems, whereas for the AOT/Brij-56/IBB system, the $\omega_{0,max}$ varied with [S_T] (60.5–78.0). It has been reported that benzene is a very good penetrator and can interact with the ester carbonyls of AOT and dehydrate the polar groups at the surfactant–water interface, and thereby increases the solubilization of water in reverse micelles [57]. But surfactant monomers cannot be aggregated in benzene due to the strong affinity of highly polarizable benzene molecules for polyoxyethylene chains of nonionic surfactants [58]. However, the addition of a small amount of water can promote micellization by retracting aromatic hydrocarbons from the polar chain of surfactant [59,60]. Thus the solubilization of water in aromatic-oil-based reverse micellar systems can be expected to be a function of the surfactant concentration, as it has been observed for the IBB stabilized system. Increased surfactant concentration can give rise to higher micellar density, and thereby increases the solubilization capacity.

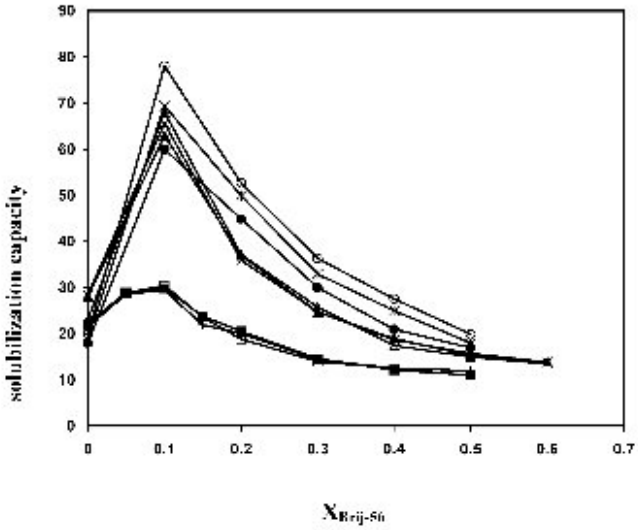

Fig. 1. Effect of surfactant concentration on solubilization of water in AOT/Brij-56/oil reverse micellar system at 303 K with $X_{Brij\text{-}56} = 0.1$. 1. IPM: (□) 0.1 mol dm^{-3}; (+) 0.175 mol dm^{-3}; (■) 0.25 mol dm^{-3}; 2. Cy: (△) 0.1 mol dm^{-3}; (×) 0.175 mol dm^{-3}; (▲) 0.25 mol dm^{-3}; 3. IBB: (○) 0.1 mol dm^{-3}; (∗) 0.175 mol dm^{-3}; (●) 0.25 mol dm^{-3}.

3.1.2. Solubilization of water in IPM-based systems

AOT reverse micellar systems with 0.1 mol dm^{-3} surfactant concentration in IPM have been observed to solubilize a substantial amount of water, ω_0 (=[water]/[surfactant]) ~ 22. The addition of nonionic surfactants of different chemical structures (Brijs, Tweens, Spans, Igepal) to AOT/IPM (at a fixed [S_T] of 0.1 mol dm^{-3}) has been observed to enhance the maximum solubilization capacity. The solubilization capacities of AOT + nonionic systems are observed to increase with increasing nonionic content in a mixture of AOT + nonionic(s), and then decrease after passing through maxima ($\omega_{0,max}$). These results are presented in Fig. 2A. Such synergism in anionic + nonionic mixed reverse micellar systems has been attributed to coulombic, ion–dipole, or hydrogen-bonding interactions among the polar groups [45]. Brij-35 (HLB, 16.9) is more hydrophilic than Brij-30 (HLB, 9.7), since they contain the same number of methylene groups (12) in their hydrophobic moiety, but 23 and 4 ethylene oxide (EO) chains in their hydrophilic parts, respectively. It has been observed that $\omega_{0,max}$ occurs

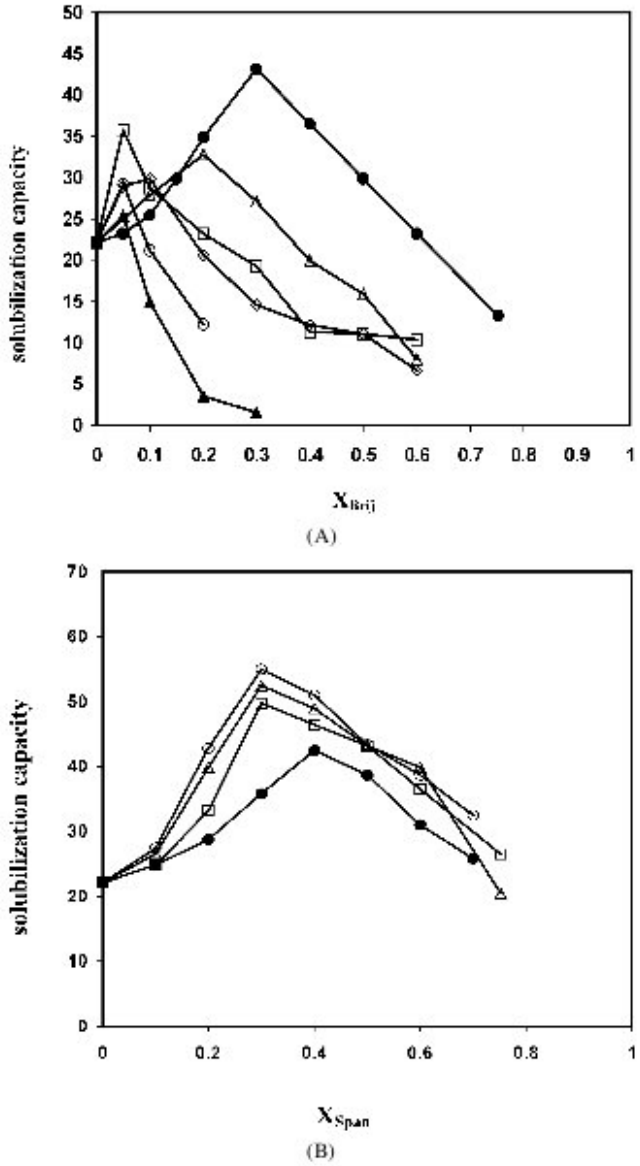

Fig. 2. (A) Solubilization capacity of water in AOT/nonionic/IPM reverse micellar system at 303 K with total surfactant concentration 0.1 mol dm^{-3} (□) AOT/Brij-76; (△) AOT/Brij-30; (◇) AOT/Brij-56; (●) AOT/Brij-52; (▲) AOT/Brij-35; (○) AOT/Brij-58. (B) Solubilization capacity of water in AOT/Span/IPM reverse micellar system at 303 K with total surfactant concentration 0.1 mol dm^{-3} in oil. (●) Span-20; (□) Span-40; (△) Span-60; (○) Span-80.

at $X_{\text{Brij-30,max}} = 0.2$ and $X_{\text{Brij-35,max}} = 0.05$ (Fig. 2A); i.e., nonionic surfactants with larger polar head group produce solubilization maximum at lower $X_{\text{nonionic,max}}$ values. The same trend is obtained for the AOT/Brij-52 [$C_{16}(EO)_2$], Brij-56 [$C_{16}(EO)_{10}$], and Brij-58 [$C_{16}(EO)_{20}$] systems with the corresponding $X_{\text{nonionic,max}} = 0.3$, 0.1, and 0.05 respectively. $\omega_{0,\max}$ is higher for the AOT/Brij-52 system (43.2) in comparison to the other two systems (30.0 and 29.0, respectively). Brij-76 contains the same number of ethylene oxide chains (10) as that of Brij-56 with almost identical HLB numbers (12.4 and 12.9, respectively), but it contains two more methylene groups in the hydrophobic part. The

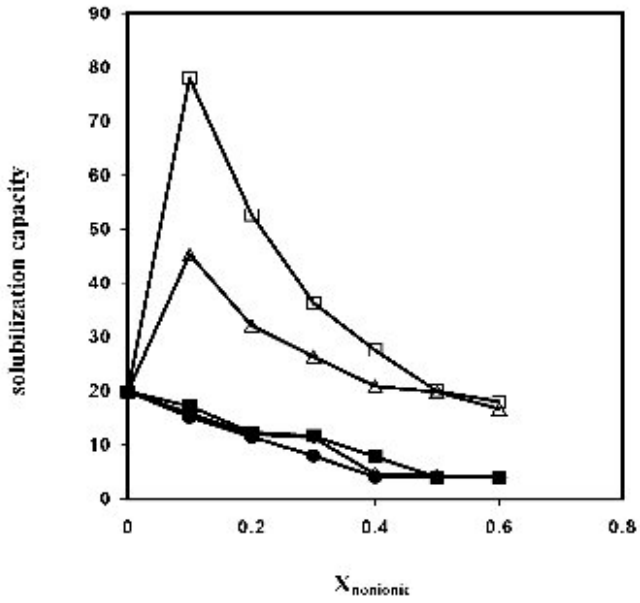

Fig. 3. Solubilization capacity of water in AOT/nonionic/IBB reverse micellar system at 303 K with total surfactant concentration 0.25 mol dm^{-3} in oil. (□) AOT/Brij-56; (△) AOT/Brij-58; (◇) AOT/Brij-52; (■) AOT/Span-40; (●) AOT/Span-60.

AOT/Brij-76 system exhibits a higher $\omega_{0,\max}$ (35.8) compared to AOT/Brij-56 (30.0) at $X_{\text{nonionic,max}} = 0.05$, which is identical with the AOT/Brij-35 and AOT/Brij-58 systems.

Four different Spans (viz. Span-20, -40, -60, and -80) (lipophilic nonionic surfactants, sorbitan fatty acid esters) are blended with AOT in IPM at a fixed [S_T] of 0.1 mol dm^{-3}, and water solubilization behavior has been studied. The solubilization capacity of water in mixed systems with mole fraction of Spans is shown in Fig. 2B. The Spans have identical polar head groups (sorbitan esters), but they differ in their hydrocarbon chain length. $\omega_{0,\max}$ has been obtained at $X_{\text{nonionic,max}} = 0.4$ for the AOT/Span-20 systems, whereas for the other three systems $\omega_{0,\max}$ are obtained at $X_{\text{nonionic,max}} = 0.3$. Unlike other nonionic surfactants, Spans do not contain any POE chain. Span-20 has the smallest hydrocarbon tail part (lauric acid side chain on the sorbitan ring) and its HLB value is 8.6. Span-20 is expected to be the most polar among the studied Span series with HLB values of 6.7, 4.7, and 4.3, respectively. AOT/Span-20 blend produces $\omega_{0,\max}$ at a higher $X_{\text{nonionic,max}}$ than the other three AOT/Span systems. This result is not consistent with other nonionic surfactants containing EO chains. The interfacial behavior of Spans varies as a result of differences in molecular structure and hydrophobicity. Since the hydrophilic portion of all the Spans are similar, it may be reasoned that the interactions between the fatty acid portions of the Spans are the main contributors to the differences in the interfacial elasticities as a consequence of interfacial packing [61]. However, $\omega_{0,\max}$ value increases with increased hydrophobicity of the tail part of the Spans and follows the order Span-80 (55.0) > Span-60 (52.5) > Span-40 (50.0) > Span-20 (42.4). Similar observations have been

Table 1
Solubilization of water ($\omega_{0,max}$) in mixed reverse micellar systems: (A) anionic–nonionic; (B) cationic–nonionic; (C) nonionic–nonionic in different oils at 303 K

Surfactant	IPM[a,d,g] $\omega_{0,max}$[j]	IBB[b,e,h] $\omega_{0,max}$	Cyclohexane[c,f,i] $\omega_{0,max}$
	(A) AOT/nonionic(s)/water; $[S_T] = 0.1$ mol dm^{-3} (0.25 mol dm^{-3} for IBB)		
Brij-30	32.8 (0.2)	–	–
Brij-35	25.4 (0.05)	35.7 (0.1)	33.3 (0.1)
Brij-52	43.2 (0.3)	N	N
Brij-56	30.0 (0.1)	60.5 (0.1) with $[S_T] = 0.1$ mol dm^{-3} 78.0 (0.1) with $[S_T] = 0.25$ mol dm^{-3}	68.0 (0.1)
Brij-58	29.0 (0.05)	39.0 (0.1) $[S_T] = 0.1$ mol dm^{-3} 45.3 (0.1) $[S_T] = 0.25$ mol dm^{-3}	36.4 (0.1)
Brij-76	35.8 (0.05)	–	–
Tween-20	27.3 (0.05)	57.5 (0.1)	84 (0.05)
Tween-40	30.0 (0.05)	57.0 (0.1)	79.0 (0.05)
Span-20	42.5 (0.4)	N	N
Span-40	50.0 (0.3)	N	N
Span-60	52.5 (0.3)	N	N
Span-80	55.0 (0.3)	N	N
Igepal CO 520	47.4 (0.2)	59.6 (0.6)	98.6 (0.4)
	(B) DDAB/nonionic(s)/oil/water; $[S_T] = 0.1$ mol dm^{-3}		
Brij-52	N	N	N
Brij-56	30 (0.3)	N	48.4 (0.5)
Brij-58	39.5 (0.1)	48.0 (0.2)	40.7 (0.4)
Span-40	N	N	N
Span-60	N	N	N
Igepal CO 520	22.0 (0.8)	–	23.5 (0.8)
	(C) Igepal CO 520/nonionic(s)/oil/water; $[S_T] = 0.1$ mol dm^{-3}		
Brij-52	N	N	N
Brij-56	N	17.8 (0.5)	57.0 (0.2)
Brij-58	N	11.3 (0.1)	33.7 (0.2)
Span-40	N	N	N
Span-60	N	N	N

Note. N indicates that no maximum in solubilization was observed.
[a] $[\omega_0] = [\text{water}]/[\text{AOT}]$ in IPM at $[S_T] = 0.1$ mol dm^{-3} is equal to 22.13 at 303 K.
[b] $[\omega_0]$, same in IBB at $[S_T] = 0.25$ mol dm^{-3} is equal to 19.9 at 303 K.
[c] $[\omega_0]$, same in Cy at $[S_T] = 0.1$ mol dm^{-3} is equal to 20.2 at 303 K.
[d] $[\omega_0] = [\text{water}]/[\text{DDAB}]$ in IPM at $[S_T] = 0.1$ mol dm^{-3} is equal to 7.7 at 303 K.
[e] $[\omega_0] = [\text{water}]/[\text{DDAB}]$ in IBB at $[S_T] = 0.1$ mol dm^{-3} is equal to 6.6 at 303 K.
[f] $[\omega_0] = [\text{water}]/[\text{DDAB}]$ in Cy at $[S_T] = 0.1$ mol dm^{-3} is equal to 15.1 at 303 K.
[g] $[\omega_0] = [\text{water}]/[\text{Igepal CO 520}]$ in IPM at $[S_T] = 0.1$ mol dm^{-3} is equal to 5.5 at 303 K.
[h] $[\omega_0] = [\text{water}]/[\text{Igepal CO 520}]$ in IBB at $[S_T] = 0.1$ mol dm^{-3} is equal to 4.8 at 303 K.
[i] $[\omega_0] = [\text{water}]/[\text{Igepal CO 520}]$ in Cy at $[S_T] = 0.1$ mol dm^{-3} is equal to 25.0 at 303 K.
[j] $\omega_{0,max}$ represents the maximum solubilization of water at a particular mole fraction of nonionic surfactant, ($X_{nonionic}$) given in the parentheses.

reported by Shah and co-workers [25] for the AOT/Span-20, Span-40, Span-60/hexadecane/water system.

Tween-20 and -40 (ethoxylated derivatives of sorbitan esters) belong to an interesting family of surfactants. The substitution of the hydroxyl groups on the sorbitan ring with polyoxyethylene groups increases the hydrophilicity of these surfactants. The HLB values of both of these Tweens (16.7 and 15.6, respectively) are comparable with those of Brij-35 and Brij-58. The solubilization behaviors of AOT/Tween-20 and AOT/Tween-40 systems have been found to be almost identical to those of AOT/Brij-35 and AOT/Brij-58 blended systems with $X_{Tween,max} = 0.05$ and $\omega_{0,max}$ values of 27.3 and 30.0, respectively (figure not shown).

Solubilization capacity of cationic DDAB in IPM is relatively low ($\omega_0 \sim 8$) with 0.1 mol dm^{-3} surfactant in oil. But the blends of DDAB with nonionic surfactants (Brij-56 and Brij-58) in IPM have shown manyfold enhancement in $\omega_{0,max}$ (30.0 and 39.5) at $X_{nonionic,max} = 0.3$ and 0.1, respectively (figure not shown). Both of these systems exhibit synergism in solubilization of water at a lower mole fraction for more hydrophilic surfactant, Brij-58 as compared to that of Brij-56. The size of the polar head group of the non-

ionic(s), as indicated by the number of EO chains present in the respective surfactant, plays a significant role in the solubilization process of water in these systems too. DDAB blended with Span-40, Span-60, and Brij-52 in IPM, however, does not exhibit any increase in solubilization of water.

The nonionic surfactant Igepal CO 520 (C_9PhE_5, nonylphenyl ethoxylate) has been reported to solubilize a substantial amount of water in hydrocarbon oils (Cy + *n*-hexane, 1:1, v/v) [38]. In the present study, maximum solubilization of water in DDAB/Igepal CO 520/IPM mixed system is rather low ($\omega_{0,\max}$; 22.0) at $[S_T] = 0.1$ mol dm^{-3} and is obtained at high content of Igepal ($X_{\text{nonionic},\max} = 0.8$) (figure not shown). Igepal CO 520 contains five EO chains with HLB value of 10.0. The differences in respect of size of the polar head group and hydrophobic moiety between two classes of nonionic surfactants (Brijs and Igepal) as well as the bulkier head group size of DDAB may be the reason for obtaining such values. No synergism in solubilization of water has been observed for Igepal/Brijs and Igepal/Spans mixed systems in IPM.

3.1.3. Solubilization of water in Cy-based systems

Solubilization capacity of mixed surfactant reverse micellar systems (AOT/nonionic) in Cy has been examined with $[S_T]$ of 0.1 mol dm^{-3}. It has been observed that solubilization capacity passes through maximum for AOT/Brij-56, AOT/Brij-58, AOT/Tween-20, AOT/Tween-40 systems with corresponding $X_{\text{nonionic},\max} = 0.1$, 0.1, 0.05, 0.05 respectively. On the other hand, no maximum in solubilization capacity has been observed for AOT/Brij-52 and AOT/Span systems, instead solubilization of water decreases steadily with increasing nonionic content in the blend (figure not shown). $\omega_{0,\max}$ values are observed to be higher than those obtained with IPM oil, whereas identical $X_{\text{nonionic},\max}$ values have been obtained except for the AOT/Brij-58 system. DDAB/Brij-56 and DDAB/Brij-58 mixed systems in Cy also exhibit a maximum solubilization capacity with $[S_T]$ of 0.1 mol dm^{-3}. Higher $\omega_{0,\max}$ value (48.4) is observed for DDAB/Brij-56 system as compared to the DDAB/Brij-58 system (40.7) and the corresponding $X_{\text{nonionic},\max}$ values are 0.5 and 0.4, respectively. Such synergism is not observed for DDAB/nonionic (Brij-52, Spans) systems.

Among the mixed nonionic (Igepal CO 520)–nonionic (Brijs and Spans) systems in Cy, Igepal/Brij-56 and Igepal/Brij-58 blends are observed to show synergism ($\omega_{0,\max}$ 57.0 and 33.7) at $X_{\text{nonionic},\max} = 0.2$ for both the systems, whereas for Igepal/Brij-52, Span-40, and Span-60 mixed systems, solubilization capacity decreases as the content of the nonionic surfactant increases in the mixture.

3.1.4. Solubilization of water in IBB-based systems

Solubilization of water in single or mixed reverse micellar systems using isobutylbenzene (IBB), an aromatic oil, is hardly reported. The AOT/IBB reverse micellar system is observed to solubilize a good amount of water with 0.1 mol dm^{-3} surfactant in oil ($\omega_0 \sim 18.0$). When a nonionic surfactant, Brij-56 is blended with AOT in IBB, the $\omega_{0,\max}$ value increases upto 60.5 at $X_{\text{Brij-56},\max} = 0.1$ and on increasing $[S_T]$ to 0.25 mol dm^{-3}, a further enhancement of $\omega_{0,\max}$ value to 78.0 is observed at $X_{\text{Brij-56},\max} = 0.1$. A similar trend is noticed for the AOT/Brij-58 system also, with relatively smaller $\omega_{0,\max}$ values of 39.0 and 45.3 with total surfactant concentrations of 0.1 and 0.25 mol dm^{-3}, respectively, but at identical $X_{\text{Brij-58},\max}$ value of 0.1. For AOT/Brij-52, AOT/Span-40, AOT/Span-60 systems, no such synergism is obtained. The results are depicted in Fig. 3. Both AOT/Tween-20 and AOT/Tween-40 systems (with surfactant concentration of 0.1 mol dm^{-3}) have shown maxima in solubilization capacity ($\omega_{0,\max}$; 57.5 and 57.0, respectively) at $X_{\text{Tween},\max} = 0.1$. In the DDAB/IBB reverse micellar system (with surfactant concentration 0.1 mol dm^{-3}), the addition of Brij-58 has been found to increase $\omega_{0,\max}$ value around sevenfold at $X_{\text{Brij-58}} = 0.1$ (figure not shown). But the Brij-56 and Brij-52 blends fail to show any synergism. When Span-40 or Span-60 is added to the DDAB/IBB system, a decrease in solubilization of water is observed with increase in the Span content in the mixture.

Igepal CO 520/IBB system (with surfactant concentration of 0.1 mol dm^{-3}) exhibits low water solubilization (ω_0, 4.8), and when Brij-52 is added as the second surfactant, it decreases further with increasing $X_{\text{Brij-52}}$. But for Igepal CO 520/Brij-56 and Igepal CO 520/Brij-58 blends in IBB, $\omega_{0,\max}$ values are obtained as 17.8 and 11.3, respectively, with corresponding $X_{\text{Brij},\max}$ of 0.5 and 0.1 respectively (figure not shown).

3.2. Comprehensive analysis of water solubilization in mixed reverse micellar systems in three oils (IPM, Cy, IBB)

3.2.1. Effect of nonionic surfactant

A comprehensive data of water solubilization for different mixed reverse micellar systems in three oils has been presented in Table 1. Solubilization of water in reverse micellar systems depends upon many factors, for example, type of surfactant (and cosurfactant/second surfactant), oil, temperature, and additives [45]. But the main driving force of such solubilization is the spontaneous curvature and the elasticity (or rigidity) of the interfacial film formed by the surfactant system [26]. If the interfacial curvature and the bending elasticity are fixed, solubilization can be maximized by minimizing the interfacial bending stress of the rigid interface and the attractive interdroplet interaction [34,35]. The critical packing parameter (CPP, given by $P = v/al$ where v and l are respectively the volume and length of the hydrophobic chain and a is the area of the polar head group of the surfactant) of the surfactant plays an important role in water solubilization.

In the present study, addition of nonionic surfactants of different types and chemical structures (Brijs, Tweens, Spans, and Igepal) to AOT/IPM/water reverse micelles produces synergism in their solubilization capacity. The highest and lowest $\omega_{0,\max}$ values are obtained with the AOT/Brij-

52 (43.2) and AOT/Brij-35 (25.4) systems, respectively, at corresponding $X_{\text{nonionic,max}}$ values of 0.3 (highest) and 0.05 (lowest). The mixed systems containing Brij-35, Brij-58, and Brij-76 exhibit $\omega_{0,\max}$ at low $X_{\text{nonionic,max}} = 0.05$, whereas for Brij-30 and Brij-56 systems, solubilization maxima are obtained at relatively higher $X_{\text{nonionic,max}}$ (= 0.2 and 0.1, respectively). For AOT/Tween systems, $\omega_{0,\max}$ follows the order Tween-40 > Tween-20 at $X_{\text{Tweens,max}} = 0.05$, whereas for AOT/Spans systems, $\omega_{0,\max}$ follows the order Span-80 > Span-60 > Span-40 > Span-20 at $X_{\text{Spans,max}} = 0.3$ (except for $X_{\text{Span-20,max}} = 0.4$). The AOT/Igepal system produces an $\omega_{0,\max}$ value of 47.4 at $X_{\text{Igepal,max}} = 0.2$. The plausible mechanism for the solubilization phenomenon in mixed reverse micelles is not straightforward, because of the interdependence of both the parameters ($\omega_{0,\max}$ and $X_{\text{nonionics,max}}$) arising out of the hydrophilic–lipophilic balance (HLB) of the added nonionic surfactant. From close scrutiny of the size (i.e., the number of POE chains) and configuration of the polar head group, hydrophobic moiety of the nonionic surfactants of various types (Scheme 1 in Supplementary Material), it can be inferred that the $\omega_{0,\max}$ values obtained in these mixed systems is primarily governed by the number of carbon atoms in the hydrocarbon moiety of the nonionic surfactant, whereas $X_{\text{nonionic,max}}$ is a function of the size and composition of the head group of the added nonionic(s). A similar trend is also obtained in DDAB/nonionic(s) blended systems. The counterbalance between these two factors plays a decisive role on the structure of the interface and continuous phase on solubilization of water in mixed reverse micelles. An explanation in support of these inferences has also been presented in the subsequent section using the model proposed by Shah et al. [25–27].

3.2.2. *Rationalization of solubilization of water in mixed reverse micelles in IPM*

The critical packing parameter CPP of the nonionic surfactant decreases with increase in EO chain length and is smaller than that of the anionic surfactant, AOT. CPP of a mixed surfactant system can be given as [62,63],

$$P = \left[(xv/al)_{\text{A}} + (xv/al)_{\text{B}}\right]/(x_{\text{A}} + x_{\text{B}}), \tag{1}$$

where x is the mole fraction of the surfactant present at the interface and the significance of the other parameters has been mentioned earlier. Eq. (1) predicts that CPP of the mixed reverse micellar system decreases with the increase of nonionic surfactant content and their EO chain lengths, and thereby leads to an increase in the droplet radius. This can affect the natural tendency of AOT to form reverse micelle and hence also the solubilization behavior. The change in the interfacial rigidity due to the addition of certain amount of nonionic surfactant is the main driving force for the observed synergism. Our observations are also supported by the argument of Nazario et al. [64]. They reported that the main driving force for water solubilization in mixed surfactant (AOT + C_iE_j, where i is the number of carbon atoms in the hydrophobic part and j is the number of EO chains in the hydrophilic part of the nonionic surfactant) reverse micellar systems is the presence of the hydrophilic group of the nonionic surfactant. On the other hand, the AOT/Brij-56 system produces $\omega_{0,\max}$ (30.0) at a higher $X_{\text{Brij-56,max}}$ (0.1) in comparison to the AOT/Brij-76 system (35.8 and 0.05, respectively), though Brij-56 and Brij-76 have the same polyoxyethylene chains (POE), but the former has a smaller hydrophobic chain length (C_{16}) than the later (C_{18}). So the contribution of hydrophobic moiety can not be neglected while determining the maximum in solubilization capacity. Higher $\omega_{0,\max}$ values (range between 42.5 and 55.0) are obtained for AOT/Spans/IPM/water systems in comparison to AOT/Brijs (except for Brij-30 and Brij-52) and AOT/Tweens blended systems. The variations in both $\omega_{0,\max}$ and $X_{\text{nonionic,max}}$ for AOT/Span systems may be explained on the basis of the size of the polar head group, which decreases or limits the attractive interaction between microemulsion droplets and radius of spontaneous curvature of the interface [25–27]. Higher values of both $\omega_{0,\max}$ (47.4) and $X_{\text{nonionic,max}} = 0.2$ for the AOT/Igepal system may be due to the difference in chemical structure and lesser number of POE chains (five) than with other nonionic(s).

3.2.3. *Effect of oils*

The solubilization phenomenon in reverse micellar systems stabilized by AOT/hydrocarbons was explained on the basis of the model developed by Shah and co-workers [25–27]. According to them, the growth of microemulsion droplets during the solubilization process and consequently the phase separation in such systems is limited by two opposing factors, namely the radius of spontaneous curvature (R_0) as the result of curvature effect and the critical radius of droplets (R_c) due to the result of attractive interaction among the droplets. The curvature effect is related to the cohesive force between the hydrocarbon chains at the interface as well as to the rigidity of the interface. For such systems, the solubilization capacity can be increased by any modification of the molecular structure of either the interface or continuos phase so that R_0 is increased. Starting from a short-chain alkane, increasing the oil chain length would gradually reduce the cohesive interaction between the hydrocarbon chains of the interface and decrease the interfacial rigidity due to decreasing oil penetration. The solubilization for such systems thus increases due to the decrease in packing parameter (P) and consequent increase in natural radius. On the other hand, for systems with greater chain length alkanes, the interdroplet interaction governs the solubilization process. Consequently one would expect a decrease in solubilization in microemulsion with further increase in oil chain length. At the point of oil chain length compatibility, both of these interactions are minimized; hence a maximum solubilization results. They showed that in an AOT/alkane/water system, solubilization capacity increases with increase in the oil chain length from benzene to heptane and then decreased on further increase of chain length upto hexadecane.

They concluded that the ascending part of this solubilization maximum is due to the curvature effect (with oils of short chain length) and the descending part is due to the interdroplet interaction effect (with oils of higher chain length). This model predicts that at a given surfactant concentration, the maximum solubilization capacity of the system can be obtained by adjusting the interfacial curvature and elasticity to optimum values at which the bending stress and the attractive forces of the interface are both minimized. Hence, one can increase the solubilization of a microemulsion with a rigid interface by increasing its natural radius and fluidity of the interface. On the other hand, the solubilization of a microemulsion of a fluid interface can be increased by increasing the interfacial rigidity and decreasing the natural radius.

In the present study, phase separation upon the addition of excess water in AOT/oil/water reverse micellar systems has been examined with the help of dye solubilization process for these three oils. It was found that for all these systems, a small volume of lower phase coexisted with a larger volume of upper phase after complete phase separation. When an oil-soluble dye, Sudan IV, was added into these systems, the lower phase remained colorless, whereas the upper phase became intensely red. On the other hand, on addition of a water-soluble dye, Eosin Blue, the upper phase became faintly violet, whereas the lower phase turned intensely violet. These observations strongly support the fact that the lower phase is a pure aqueous phase in equilibrium with an upper microemulsion phase (Winsor II system). Such a phase separation indicates that the curvature effect governs the solubilization phenomenon in these studied systems. Such type of phase separation is likely to be observed in AOT reverse micellar systems stabilized in hydrocarbon oils with low molar volume (<150 cc mol^{-1}) [25]. In the present study, for AOT/Cy/water and AOT/IBB/water systems, such phase separation is quite likely to occur, but for IPM oil (consisting of large hydrocarbon tail and hydrophilic ester group) with high molar volume (317 cc mol^{-1}), this type of phase separation is quite unusual. For hydrocarbon oils with high molar volume (>150 cc mol^{-1}), interdroplet interaction plays the governing role in solubilization phenomenon and a Winsor I type phase separation (in which a lower microemulsion phase remains in equilibrium with an excess upper oil phase) is likely to be observed. The anomalous behavior of AOT/IPM/water system supports the fact that not only the molar volume of oils, but other factors like polarity, viscosity, molecular structure, etc., of oils may also play key roles in solubilization behavior of AOT/oil/water reverse micellar systems [25,26,29,30].

AOT/Brij-56 blend exhibits maximum in solubilization capacity in all the three oils at $X_{\text{nonionic,max}} = 0.1$. Phase separation has also been studied for the systems AOT/Brij-56/Cy, IBB, IPM/water at $X_{\text{nonionic}} = 0.2$. It has been observed that after complete phase separation, when an oil-soluble dye, Sudan IV, was added into it, both the phases (lower and upper) became red. On the other hand, the addition of a water-soluble dye Eosin Blue turned the lower phase intensely violet, whereas the upper phase remained colorless which clearly indicates that an equilibrium between a lower microemulsion phase with an excess oil phase (Winsor I system) is established. These observations point out that interdroplet interaction plays the governing factor in determining the phase separation in these systems [25]. As evidenced earlier, curvature factor governs the phase separation of AOT reverse micellar systems in these three oils. So any factor that increases the rigidity of the interface and hence the natural radius of curvature (R), increases the solubilization capacity significantly. Incorporation of a second nonionic surfactant with large polar head group decreases the effective packing parameter (P_{eff}) (Eq. (1)) by increasing a (area of polar head group), thereby increasing R. But such an increase in R increases the interdroplet interaction, and at a certain value of $R \sim R_c$ (critical radius of curvature), the interdroplet interaction starts to govern the solubilization process and limits the solubilization capacity. Hence, for all these mixed systems, the ascending curve of the solubilization capacity is the curvature branch (R_0), whereas the descending curve is the interdroplet interaction branch (R_c). In the AOT/Brij-56/oil/water system, the $\omega_{0,\max}$ follows the trend Cy > IBB > IPM, which supports the fact that the smaller the molar volume of the oil, the larger is the effect of increasing radius of curvature, and hence higher is the solubilization capacity [65,66].

It is evident from Table 1 that AOT/Brijs (Brij-35, Brij-56, Brij-58) systems in Cy and IBB exhibit a solubilization maximum, whereas the nonionic surfactants (Brij-52, Spans) with poor hydrophilicity fail to exhibit any such maximum. AOT/Brij-56 systems in these oils produce higher $\omega_{0,\max}$ values in comparison to AOT/Brij-58 systems. Addition of nonionic surfactant with large polar head group increases the rigidity of the interface and hence increases the radius of curvature. But those with smaller polar head groups do not increase the radius of curvature significantly and hence no such synergistic effect was observed. Since Brij-58 has larger head group in comparison to Brij-56, the AOT/Brij-58 blended system reaches the critical radius of curvature (R_c) at a lower ω in comparison to AOT/Brij-56 blended system, and hence $\omega_{0,\max}$ values are observed to be higher for AOT/Brij-56 blends than for AOT/Brij-58 blends.

We have studied the solubilization behavior of AOT/nonionic (Brij-56, Brij-58, Span-60) blends in decane (Dc) oil (molar volume 195 cc mol^{-1}). The solubilization capacity of AOT/Dc/water system is governed by interdroplet interaction [23–25]. So any factor that increases the rigidity of the interface and decreases the interdroplet interaction will increase the solubilization, whereas factors that make the interface more fluid would decrease it. In the present study, AOT/Brij-56 and AOT/Brij-58 blends have not shown any synergism, whereas AOT/Span-60 blend produced a solubilization maximum at $X_{\text{nonionic,max}} = 0.3$ (figure not shown). Incorporation of nonionic surfactant with large head group (Brij-56, Brij-58) into the interface increases the fluidity of

the interface and thereby decreases the solubilization. On the other hand, Span-60 having no POE chain increases the interfacial rigidity and thereby increases the solubilization capacity. This observation is consistent with that of Shah et al. [25] wherein incorporation of Spans increased the solubilization capacity of AOT/hexadecane/water system.

Solubilization behavior and appearance of solubilization maxima in AOT/Brijs (Brij-35, Brij-56, Brij-58)/Cy, IBB, and AOT/Span-60/Dc systems follow the proposed model for solubilization [25–27]. But the solubilization behavior in IPM is unusual in this manner. AOT/IPM system exhibits phase separation due to the curvature effect, and an enhancement of solubilization capacity has been observed for both large head group nonionic surfactants (as in the case of Cy, IBB-based systems) and small head group nonionic surfactants (as in the case of Dc-stabilized system) blends. It has been reported earlier [27,29,30] that oils with high polarity can behave in a manner different from hydrocarbon oils. Zana and co-workers [29,30] showed that interdroplet interaction among the droplets is reduced for oils with high polarity which in turn can affect the solubilization process. In the present study, IPM has a higher dielectric constant (3.65) than those of Cy (2.02) and IBB (2.32). Thus the ambiguous solubilization behavior for systems stabilized in IPM may be due to its different chemical structure and comparatively higher polarity. In order to ascertain the role of molar volume of oil in the solubilization process, the solubilization behavior of AOT/Brij-56 mixed systems in two oils, 2-ethylhexanol (Eh) and eugenol (Eu), was studied. These two oils possess the same molar volume (156 cc mol^{-1}) as IBB (157 cc mol^{-1}), but differ in chemical structures and polarity. It has been observed that maximum in solubilization capacity does not occur in these two oils (Eu and Eh) and at $X_{\text{Brij}} = 0.1$, even the solubilization capacities are too low (9.3 and 11.2, respectively) as compared to that of IBB (69.4). It is evident that the molar volume of an oil is not the only key factor to influence the solubilization phenomenon in reverse micellar systems.

As salinity in w/o microemulsions is reported to affect the attractive interaction among the droplets by making the interfacial layer more rigid due to the close packing of polar groups, hence the effect of [NaCl] on the solubilization behavior in mixed reverse micellar systems would be worth while.

3.3. Influence of [NaCl] on solubilization behavior of water in mixed surfactant reverse micelles in IPM, Cy, and IBB

3.3.1. AOT/nonionics/NaCl (aqueous) in oils at a fixed composition of the nonionic(s)

The AOT/IPM/aqueous NaCl system has been observed to show a small increase in the $\omega_{\max}$ [molar ratio of aqueous NaCl to surfactant(s), 26.5] compared to that of water ($\omega_0 = 22$) at a NaCl concentration of 0.02 mol dm^{-3}. Solubilization capacity of aqueous NaCl in mixed reverse micellar systems, AOT/nonionic(s)/IPM, with total surfactant

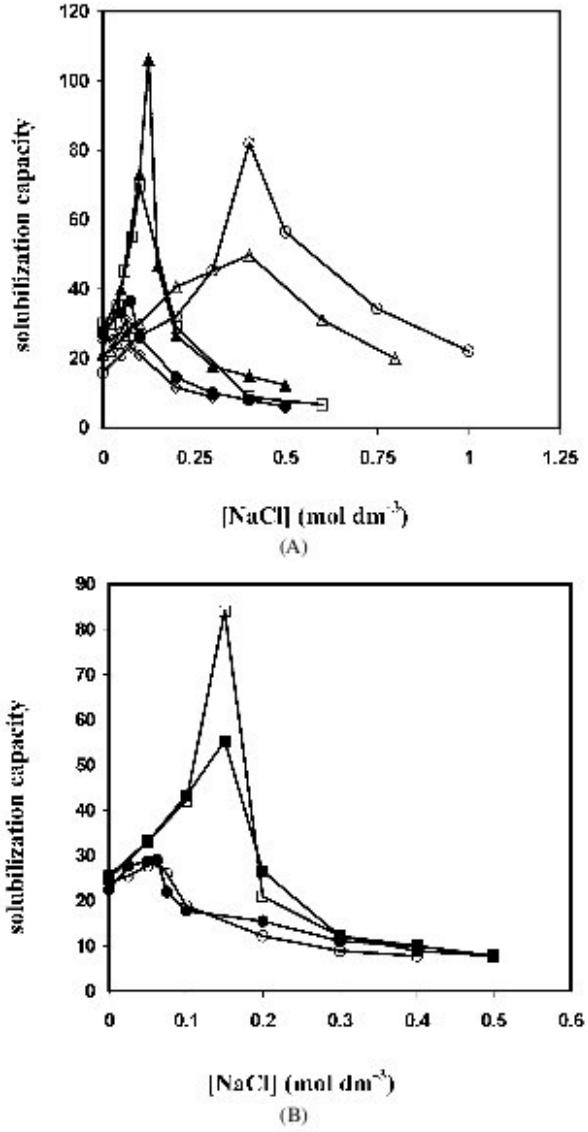

Fig. 4. Solubilization of aqueous NaCl in AOT/nonionic/IPM reverse micellar system at 303 K with surfactant concentration of 0.1 mol dm^{-3} in oil and $X_{\text{nonionic}} = 0.1$. The nonionic surfactants used: (A) (●) Brij-30; (○) Brij-35; (■) Brij-52; (△) Brij-56; (▲) Brij-58; (□) Brij-76; (B) (■) Tween-20; (□) Tween-40; (○) Span-20; (●) Span-80.

concentration of 0.1 mol dm^{-3} in oil and at $X_{\text{nonionic}} = 0.1$ at 303 K has been represented in Figs. 4A (for Brij series) and 4B (for Spans and Tweens). For all these mixed systems, solubilization capacity passes through a maximum at a threshold NaCl concentration, $[\text{NaCl}]_{\max}$. It has been further observed that solubilization maximum shifted towards a higher $[\text{NaCl}]_{\max}$ with increasing hydrophilicity of the nonionic surfactant depending upon the type and head group configuration of the nonionic surfactants. The maximum solubilization capacity of water ($\omega_{0,\max}$), NaCl ($\omega_{\max}$) and the corresponding $[\text{NaCl}]_{\max}$ in IPM-based systems are presented in Table 2. From Table 2 it has also been evident that for the AOT/nonionic blends with larger polar head group (viz. AOT/Brij-35, AOT/Brij-56, AOT/Brij-58, AOT/Brij-76, AOT/Tweens), $\omega_{\max}$ value increased manyfold in com-

Table 2
Solubilization of NaCl (ω_{max}) in mixed reverse micellar systems stabilized by AOT and different nonionic surfactants in different oils with $[S_T] = 0.1$ mol dm^{-3} and $X_{nonionic} = 0.1$ at 303 K

	IPM			IBB			Cy		
	$\omega_{0,max}$	$[NaCl]_{max}$	ω_{max}	$\omega_{0,max}$	$[NaCl]_{max}$	ω_{max}	$\omega_{0,max}$	$[NaCl]_{max}$	ω_{max}
Brij-30	27.5	0.075	36.5	–	–	–	–	–	–
Brij-35	16.0	0.4	82.0	–	–	–		–	–
Brij-52	25.0	0.0625	31.0	20.0	N	N	19.0	N	N
Brij-56	30.0	0.1	70.0	60.0	N	N	68.0	0.025	84.0
Brij-58	21.0	0.4	50.0	39.0	0.0625	99.5	36.4	0.1	125.0
Brij-76	27.7	0.125	106	–	–	–	–	–	–
Tween-20	25.0	0.15	55.0	57.5	0.025	77.0	66.1	0.025	83.0
Tween-40	25.5	0.15	84.0	58.0	0.025	82.0	66.4	0.025	110.0
Span-20	24.0	0.0625	29.0	10.7	N	N	23.2	N	N
Span-80	23.0	0.0625	29.0	–	–	–	–	–	–

Note. N indicates that gradual decrease in solubilization of water with addition of NaCl.

parison to water, whereas for blends with smaller polar head group (viz. AOT/Brij-52, AOT/Brij-30, AOT/Spans), the increase is marginal. This result is consistent with earlier works [45] for mixed reverse micellar systems containing Brij-30, Brij-52, Brij-56, Brij-58 blends in AOT using hydrocarbon oils (Cy, *n*-hexane, *n*-heptane, *n*-octane, and isooctane).

Solubilization capacity of some selected AOT/nonionic blended systems in Cy and IBB in presence of NaCl has been studied for comparison with IPM and the results are presented in Table 2. Among the AOT/Brijs (Brij-52, Brij-56, Brij-58) blended systems, AOT/Brij-52 and AOT/Brij-56 systems in IBB, and AOT/Brij-52 in Cy have not shown any synergism, whereas the other blends exhibit solubilization maxima. For AOT/Brij-58 blend in these oils, $\omega_{0,max}$ follows the sequence Cy (125.0) > IBB (99.5) > IPM (50.0), whereas the order of $[NaCl]_{max}$ is as follows: IPM (0.4) > Cy (0.1) > IBB (0.0625). Among the Tween-based systems, Tween-40 has been found to be more influenced by NaCl as compared to the Tween-20 based system, but with identical $[NaCl]_{max}$. AOT/Spans systems stabilized in IBB and Cy do not exhibit any maximum in solubilization capacity of NaCl.

In order to gain more insight to the understanding of the solubilization phenomenon in the presence of NaCl, composition of the systems (i.e., $X_{nonionic}$) and combination of different charge types of surfactants (i.e., anionic–nonionic, cationic–nonionic, and nonionic–nonionic) are varied in mixed reverse micelles and the results are presented in the subsequent section.

3.3.2. AOT/nonionic(s)/NaCl (aqueous) in oils at different compositions of the nonionics

The effect of NaCl on the solubilization capacity of AOT/Brijs blended systems in IPM (AOT/Brij-52, Brij-56, and Brij-58) with total surfactant concentration of 0.1 mol dm^{-3} and at different $X_{nonionic}$ values, which also includes $X_{nonionic,max}$, has been studied. A representative Fig. 5A is depicted for the AOT/Brij-58 blended system. It has been observed that solubilization capacity passes through a maximum at $X_{nonionic,max} = 0.05$ for the AOT/Brij-58/IPM system. The $[NaCl]_{max}$ is found to be 0.15 mol dm^{-3} with $\omega_{max} = 70.0$. On the other hand, at $X_{nonionic} = 0.3$ ($> X_{nonionic,max}$), solubilization has been observed to be very low (~7.0) (even far below the AOT/IPM system) and then decreases steadily. Thus the effect of NaCl is more pronounced at $X_{nonionic,max}$ than other compositions, i.e., beyond $X_{nonionic,max}$. For the blend AOT/Brij-56, the solubilization capacity also passes through a maximum (ω_{max}, 70.0) at $[NaCl]_{max} = 0.1$ mol dm^{-3} at $X_{nonionic,max} = 0.1$, whereas for the composition $X_{nonionic} = 0.3$, solubilization is poorly dependent on [NaCl], and remains almost unchanged with increasing [NaCl] (figure not shown). For AOT/Brij-52 blended system, at $X_{nonionic} = 0.1$ ($< X_{nonionic,max}$), solubilization capacity passes through a maximum (ω_{max}, 34.0) at $[NaCl]_{max} = 0.04$ mol dm^{-3}. At $X_{nonionic,max} = 0.3$, a similar trend has been observed, and the corresponding ω_{max} (64.0) is found to be highest at the lowest $[NaCl]_{max}$ of 0.02 mol dm^{-3} (figure not shown). For all these mixed systems, further enhancement in solubilization has been observed in presence of NaCl at the corresponding $X_{nonionic,max}$. ω_{max} values are comparable for these mixed systems, but $[NaCl]_{max}$ depends on the content of POE chains in the nonionic surfactant. The smaller the POE chain, the lower $[NaCl]_{max}$ is required to attain ω_{max}.

In order to explain the attainment of the maximum in solubilization capacity–[NaCl] profile in mixed reverse micellar systems, we have studied the solubilization capacity of AOT/Cy, AOT/IBB, and AOT/IPM in the presence of NaCl. The solubilization capacity decreases with increasing [NaCl] for Cy and IBB-based systems, whereas for the IPM-based system solubilization capacity passes through a maximum. Zana and co-workers [29,30] previously reported that for cationic surfactants in aromatic oils, solubilization of water in presence of NaCl was enhanced for systems lying in the R_c branch; whereas for those lying in the R_0 branch, no such synergism was observed. In the present study, all these three systems have been recognized as R_0 branch systems from dye solubilization experiments. Thus decrease in solubilization with [NaCl] for AOT/Cy and AOT/IBB is consistent with the findings of Zana and co-workers [29,30], whereas

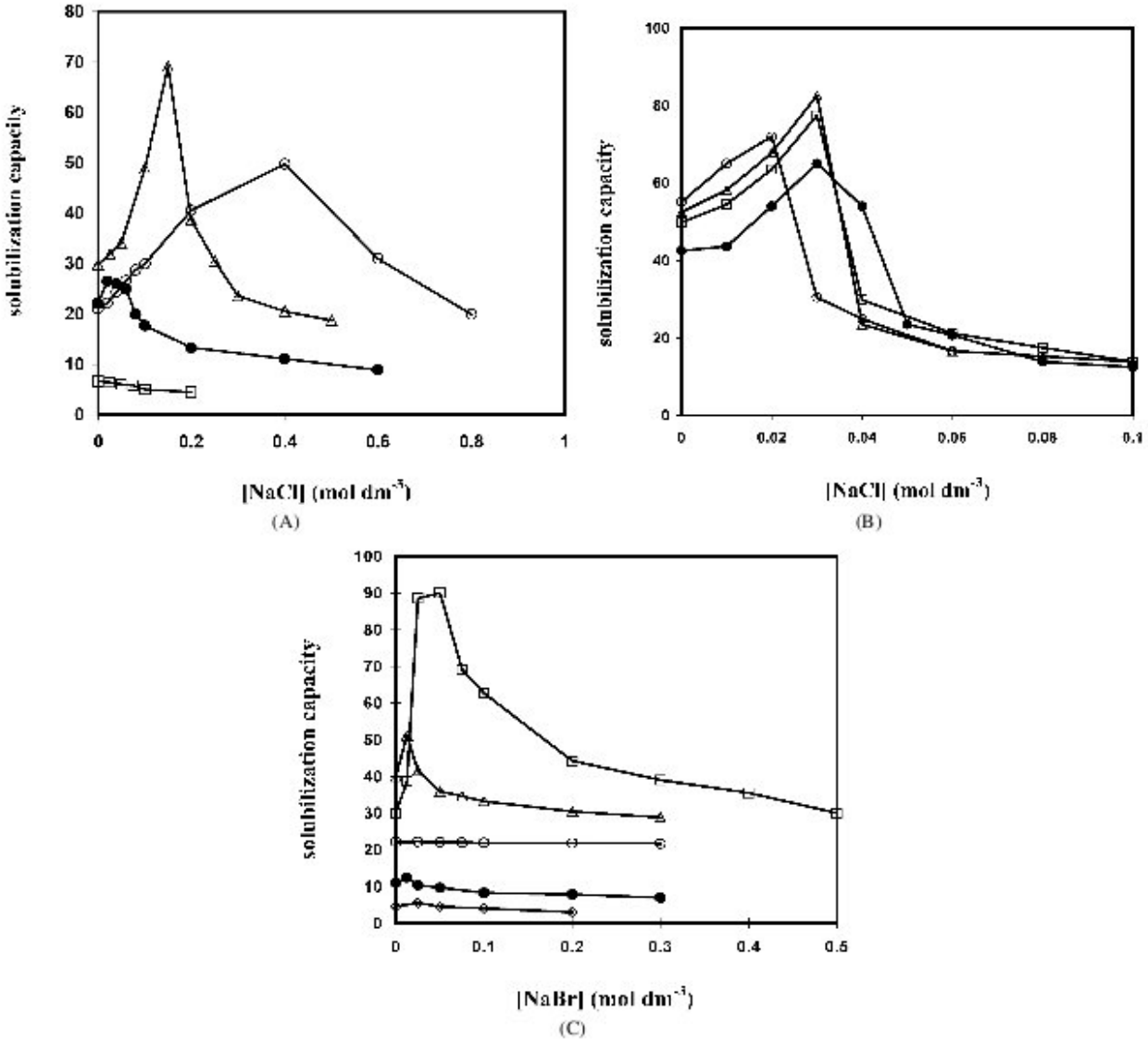

Fig. 5. (A) Solubilization of aqueous NaCl in AOT/Brij-58/IPM reverse micellar system at 303 K with surfactant concentration of 0.1 mol dm^{-3} in oil with $X_{\text{Brij-58}} = 0$ (●); 0.05 (△); 0.1 (○); 0.3 (□). (B) Solubilization of aqueous NaCl in AOT/Span/IPM reverse micellar system at 303 K with surfactant concentration of 0.1 mol dm^{-3} in oil. (●) Span-20 ($X = 0.4$); (□) Span-40 ($X = 0.3$); (△) Span-60 ($X = 0.3$); (○) Span-80 ($X = 0.3$). (C) Solubilization of aqueous NaBr in DDAB/Brij-56 (Brij-58)/IPM reverse micellar system with surfactant concentration 0.1 mol dm^{-3} in oil at 303 K. (●) No anionic, (□) Brij-56 ($X = 0.3$); (△) Brij-58 ($X = 0.1$); (○) Brij-58 ($X = 0.3$); (◇) Brij-52 ($X = 0.3$).

the results obtained for AOT/IPM system are unusual. At $X_{\text{nonionic,max}}$, the systems can be assumed to be governed by the interdroplet interaction mechanism, and the addition of NaCl into such systems can decrease such interdroplet interaction, thereby increasing solubilization. So the ascending curve of the AOT/nonionic/IPM/NaCl (aq) solubilization capacity vs [NaCl] profile has been found to be the R_c branch, whereas the descending curve as the R_0 branch. Similar results have been reported by Zana and co-workers [29,30] for cationic surfactants/aromatic oils/NaCl (aq) systems. Our results are also consistent with the findings of Derouiche and Tondre [31] for AOT/decane or dodecane/NaCl (aq) systems.

Solubilization capacity of aqueous NaCl in AOT/Span-(20, 40, 60, 80)/IPM systems with total surfactant concentration 0.1 mol dm^{-3} at $X_{\text{nonionic,max}}$ has been presented in Fig. 5B. A maximum in solubilization capacity has been observed in the solubilization capacity–[NaCl] profile for all these systems. For the AOT/Span-80 system, $\omega_{\max}$ (72.0) is obtained at $[\text{NaCl}]_{\max} = 0.02$ mol dm^{-3}, whereas for the other three systems (Span-20, Span-40, and Span-60), $[\text{NaCl}]_{\max}$ is obtained at 0.03 mol dm^{-3} with the corresponding $\omega_{\max}$ values of 65, 77.4, and 82.5, respectively. It has been reported earlier that interfacial elasticity of Span-20/hydrocarbon oil/water system increases with increasing [NaCl] and then decreases with further increase in [NaCl] [61], which may result in the observed solubilization maximum for the AOT/Span mixed systems. It may also be noted that Span-80 is the least polar surfactant among the studied Spans, and the least [NaCl] is required to bring about

the solubilization maximum among the studied AOT/Span systems.

Effect of NaCl on the solubilization capacity for AOT/Brij/cyclohexane/water mixed surfactant systems, was studied with 0.1 mol dm^{-3} surfactant concentration and at $X_{\text{nonionic, max}} = 0.1$. It has been observed that for AOT/Brij-56 and AOT/Brij-58 blends, $\omega_{\max}$ values are obtained at $[\text{NaCl}]_{\max} = 0.025$ and 0.1 mol dm^{-3}, respectively (figure not shown). AOT/Brij-58 blend produces a higher $\omega_{\max}$ (=125) as compared to the AOT/Brij-56 blend ($\omega_{\max} = 84$). However, no maximum in solubilization capacity is observed for AOT/Brij-52 blended system, the curve steadily decreases with increasing [NaCl].

For the AOT/Brij(s)/IBB systems with total surfactant concentration of 0.1 mol dm^{-3} and at $X_{\text{nonionic}} = 0.1$, it has been observed that $\omega_{\max}$ (= 99.5) is obtained at $[\text{NaCl}]_{\max} =$ 0.0625 mol dm^{-3} for the AOT/Brij-58 blended system, while for the other two mixed systems, viz. AOT/Brij-56 and AOT/Brij-52, solubilization of aqueous NaCl decreases steadily with increase in [NaCl] (figure not shown). Hence, the maximum solubilization capacity of NaCl ($\omega_{\max}$) at $X_{\text{nonionic, max}}$ in AOT/nonionic reverse micellar systems stabilized in three oils follows the same order, Cy > IBB > IPM, as in the case of solubilization of water in these mixed systems.

It can be inferred from these results that both EO chain length (or size of the polar group) and hydrophobic moiety in nonionic surfactants and their contents (i.e., composition of the surfactants in the mixture) play significant roles in determining both $\omega_{\max}$ and $[\text{NaCl}]_{\max}$.

The solubilization maximum obtained in NaCl solution can be explained on the basis of salting-in and salting-out processes [19,25,27,28,55]. Addition of electrolyte (NaCl) can expel part of the AOT molecules from the aqueous phase to the organic phase to form reverse micelle and hence solubilization increases. Addition of electrolyte decreases the interaction among the droplets by making the interfacial layer more rigid, which in turn also increases solubilization. At a higher concentration of NaCl a different phenomenon overcomes this effect. Addition of NaCl decreases the thickness of the electrical double layer of the charged interfacial film and the effective polar area of the surfactant also decreases. This in turn increases the tendency of the surfactant to form natural negative curvature, which decreases the solubilization. For blends containing nonionic surfactants with larger polar head group, the effective polar area of the surfactant at the interface is larger and hence high concentration of NaCl is required to decrease the effective polar area of the surfactant at the interface. Hence $[\text{NaCl}]_{\max}$ is high for blends containing nonionic surfactants with larger polar head groups. In an AOT-based system, the optimum NaCl concentration can be viewed as the concentration of salt just necessary so that the range of electrostatic interaction becomes such that neighboring AOT polar head groups totally ignore each other [31]. It was proposed that the Debye screening length (K^{-1}) would become smaller than the average intercharge distance between AOT molecules in the surfactant film at optimum salinity. When K^{-1} would be larger than the intercharge distance, electrostatic repulsion between AOT polar heads would give enough flexibility in the surfactant film for the droplets to be attractive. It is known that K^2 is inversely proportional to ε^{-1}, where ε is the dielectric constant of water [67]. For small droplet sizes, ε of water decreases considerably in the vicinity of the charged surface [68]. This explains the indifferent effect of NaCl on solubilization behavior of AOT/Brij-56 and AOT/Brij-58 blends at $X_{\text{Brij}} = 0.3$, where the droplet sizes can be assumed to be small.

3.3.3. DDAB/nonionics/NaBr (aqueous) in IPM at different compositions of the nonionics

No significant effect of NaBr on the solubilization behavior of the DDAB/IPM/water system has been observed. The effect of NaBr on the solubilization capacity has been examined for the mixed systems DDAB/Brij-52, Brij-56, Brij-58/IPM with total surfactant concentration 0.1 mol dm^{-3} and at different X_{nonionic}, and the results are depicted in Fig. 5C. For DDAB/Brij-56 blended system $\omega_{\max}$ (90) is obtained at $X_{\text{Brij-56,max}} = 0.3$ and the corresponding $[\text{NaBr}]_{\max}$ is 0.05 mol dm^{-3}. $\omega_{\max}$ (~51.0) is obtained at $X_{\text{Brij-58,max}} =$ 0.1 for DDAB/Brij-58 system, with the corresponding $[\text{NaBr}]_{\max}$ of 0.0125 mol dm^{-3}. At $X_{\text{Brij-58}} = 0.3$, [NaBr] shows a negligible effect on solubilization, and solubilization capacity remains almost constant (~22.0) up to [NaBr] = 0.3 mol dm^{-3}. The enhancement of solubilization capacity of DDAB/Brij systems at their corresponding $X_{\text{Brij,max}}$ can also be explained on the basis of salting-in and salting-out mechanisms as has been discussed for the AOT/Brijs blends in the previous section. On the other hand, solubilization is very poor (even remaining below the DDAB/IPM system) for DDAB/Brij-52 blend at $X_{\text{Brij-52}} =$ 0.3. In this system, the droplet sizes might be assumed to be small at relatively smaller solubilization capacity (ω) values and thus the efficiency of NaBr to affect the solubilization behavior can be assumed to be poor as discussed in the previous section.

A nonionic–nonionic blend, Igepal CO 520/Brij-56/IPM has shown almost no effect with increasing NaCl concentration (figure not shown).

3.4. Conductometric studies

In this section, an attempt has been taken up to correlate the maximum water/electrolyte solubilization with percolation of conductance in mixed reverse micelles. Percolation of conductance study extracts information about the nature of interaction among the droplets in microemulsion/reverse micellar systems. If the droplets are of noninteracting hard sphere type, no significant increase in conductance occurs with increasing water content at constant temperature or with increase in temperature at fixed water content. But if the interfaces of the droplets are fluid enough to coalesce during these collisions followed by material exchange and fusion,

a sharp rise in conductance is evidenced. This phenomenon is called percolation of conductance [69]. Percolation signifies the increase in droplet size, attractive interaction among droplets and exchange rate of materials between the droplets [70–72]. In the present investigation, conductance studies have been carried out for mixed surfactant reverse micellar systems wherein solubilization maxima ($\omega_{0,\max}$ or $\omega_{\max}$) are observed. The samples from both sides of the corresponding maxima, i.e., from the ascending branches and the descending branches are chosen.

3.4.1. Water/mixed surfactants/oil(s)

It is evident from Table 1 that the solubilization maximum ($\omega_{0,\max}$) for the AOT/Brij-56 and Brij-58 blends in Cy is obtained at $X_{\text{nonionic},\max} = 0.1$. The conductivity remains low and almost unchanged with increasing water content upto phase separation in all these systems. No percolation is evidenced on increasing $[S_T]$ from 0.1 to 0.25 mol dm^{-3} (figure not shown). AOT/Cy/water system has earlier been reported to be nonpercolating [73]. Cy has a low molar volume and hence can penetrate deep into the interfacial layer to make the interface rigid and hard sphere type. This makes the system nonpercolating. Incorporation of a second nonionic surfactant into AOT/Cy/water also fails to make the system to percolate.

AOT/Brij-56, Brij-58/IBB/water systems exhibit solubilization maxima at $X_{\text{nonionic},\max} = 0.1$ (Table 1). The conductivity of AOT/Brij-56 mixed systems at different $X_{\text{Brij-56}}$ as a function of ω is depicted in Fig. 6A. The shaded regions in the solubilization capacity vs X_{nonionic} profile represent the percolation range for both the systems (Fig. 6B). No percolation is observed in the ascending branch of the solubilization maximum. The system behaves as hard sphere droplets. On the other hand, samples chosen from the descending branch exhibit ω-induced percolation in conductance. From these observations it is suggested that the descending branch is composed of droplets with fluid interfaces, and the interdroplet interaction, which governs the solubilization phenomenon as discussed in the earlier sections, is confirmed. It has also been found that the percolation threshold (ω_p) decreases with increased X_{Brij}. Addition of Brijs increases the droplet radius by decreasing the packing parameter, which in turn facilitates the droplet coalescence that limits the solubilization capacity. It can be noted that Brij-58 has a greater influence on decreasing ω_p than that of Brij-56 and may be due to the larger size of the polar head group [55].

The blends of AOT/Brij-52, Brij-56, and Brij-58 in IPM and water exhibit solubilization maxima at $X_{\text{nonionicm},\max} = 0.05$, 0.1, and 0.3, respectively (Table 1). Fig. 7A depicts the conductivity of AOT/Brij-52 mixed systems at different $X_{\text{Brij-52}}$ as a function of ω. The shaded regions in the solubilization capacity vs X_{nonionic} profile represent the percolation range for all the mixed systems (Fig. 7B). It has been found that conductivity remains low and practically unchanged for systems chosen from the ascending branch,

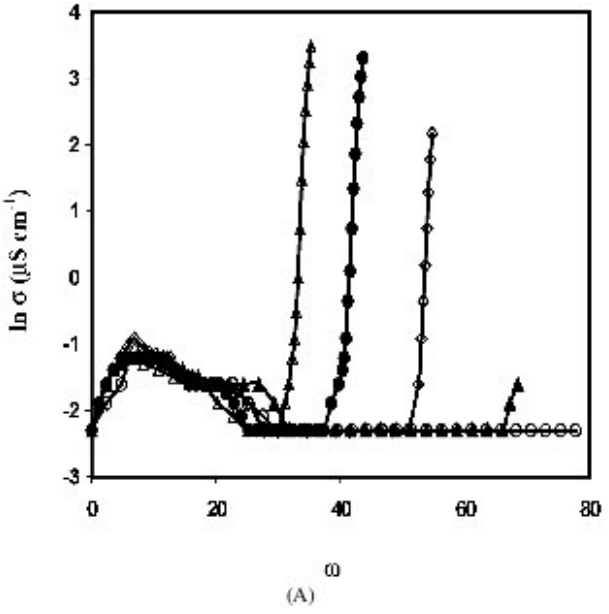

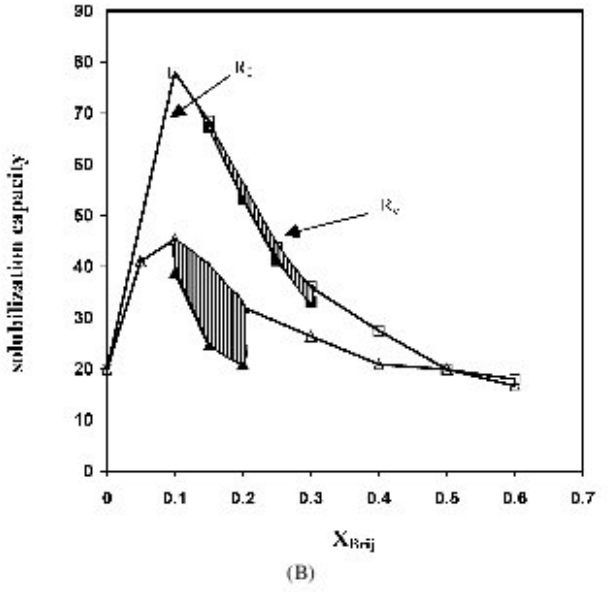

Fig. 6. (A) Conductance study and percolation region of the system AOT/Brij-56/IBB/water at 303 K with surfactant concentration 0.25 mol dm^{-3}. (○) $X = 0.1$; (▲) $X = 0.15$; (◇) $X = 0.2$; (●) $X = 0.2$; (△) $X = 0.3$. (B) The shaded portion represents the percolation region. (△) AOT/Brij-58; (□) AOT/Brij-56. R_0 indicates the curvature branch and R_c indicates the interdroplet interaction branch.

which confirms their hard-sphere type droplet nature. Percolation of conductance has been observed for all the mixed systems, which lie along the descending branch. A similar trend is also observed for the blends, AOT/Brij-76, AOT/Tween-40, AOT/Igepal CO 520, and AOT/Span-60 stabilized in IPM (not exemplified). In AOT/nonionic(s)/IPM systems, ω_p decreases with increasing X_{nonionic} as in the case of AOT/Brij/IBB systems. DDAB/Brij-56 and DDAB/Brij-58 blends in IPM also exhibit similar results with the ascending curve as the non-percolating one and the descending curve as the percolating one. Conductivity of DDAB/

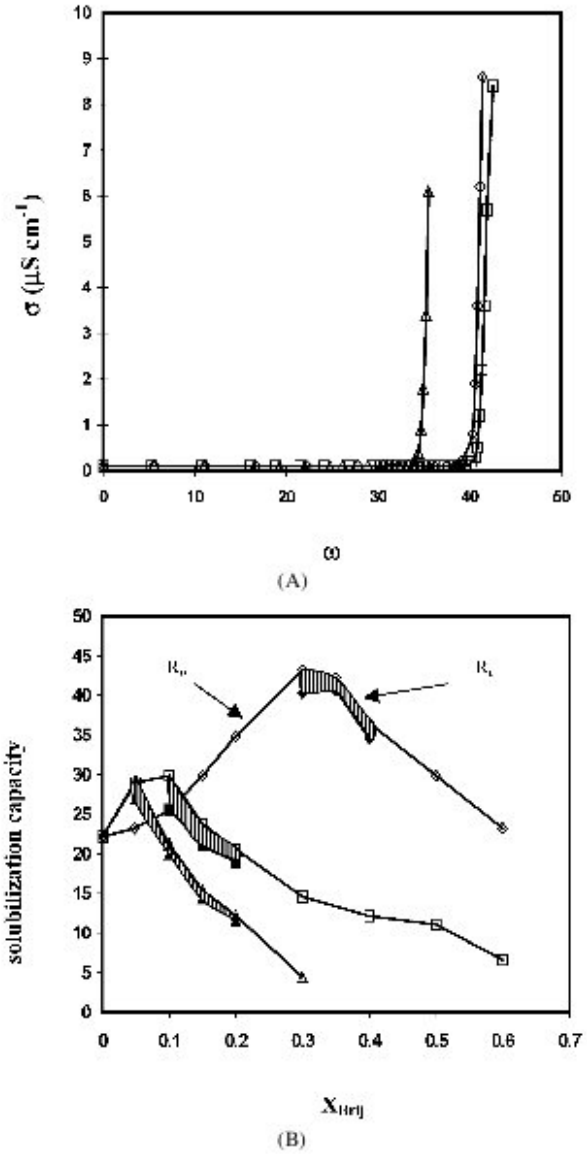

Fig. 7. Conductance study and percolation region of the system AOT/Brij/IPM/water at 303 K with total surfactant concentration 0.1 mol dm^{-3}: (A) Brij-52: (□) $X = 0.3$; (◇) $X = 0.35$; (△) $X = 0.4$. (B) Shaded portion represents percolation region: (◇) AOT/Brij-52; (□) AOT/Brij-56; (○) AOT/Brij-58. R_0 indicates the curvature branch and R_c indicates the interdroplet interaction branch.

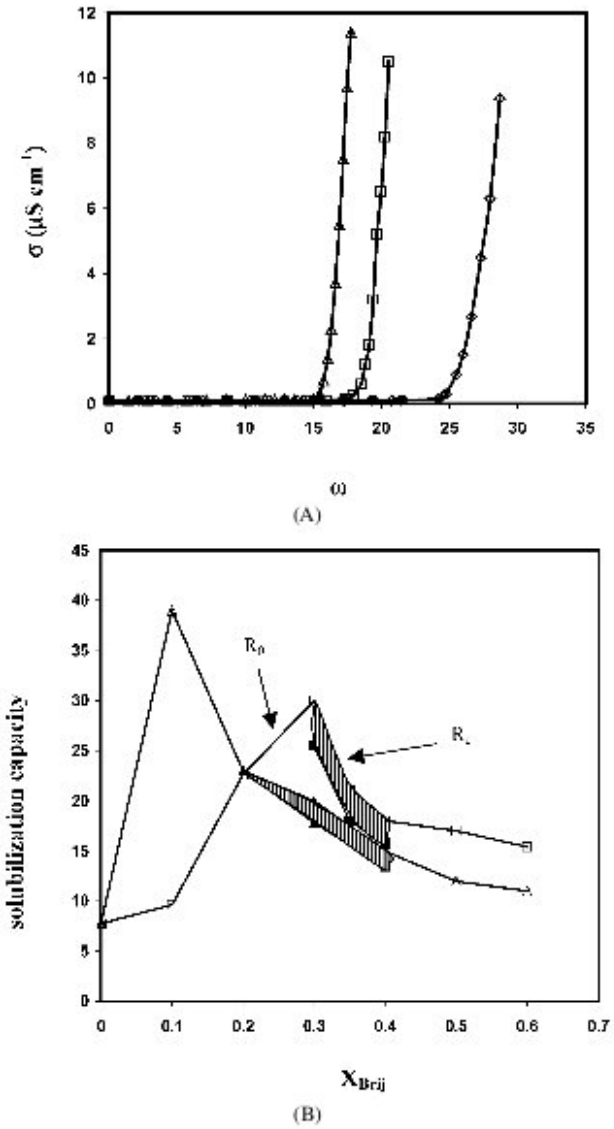

Fig. 8. Conductance study and percolation region of the system DDAB/Brij/IPM/water at 303 K with total surfactant concentration 0.1 mol dm^{-3}. (A) Brij-56: (●) $X = 0.2$; (◇) $X = 0.3$; (□) $X = 0.3$; (△) $X = 0.4$; (B) The shaded portion represents the percolation region. (△) AOT/Brij-58; (□) AOT/Brij-56. R_0 indicates the curvature branch and R_c indicates the interdroplet interaction branch.

Brij-56/IPM/water system at different X_{Brij} as a function of ω, and the corresponding percolation regions in the solubilization capacity vs X_{nonionic} profile are depicted in Figs. 8A and 8B. All these observations confirm our earlier findings that the solubilization phenomenon in the ascending branch is governed by the curvature effect (R_0), whereas that in the descending branches is governed by the interdroplet interaction effect (R_c) for AOT/nonionic and DDAB/nonionic blends in IPM. Such a phenomenon is unusual for the IPM oil-based system so far as its high molar volume is concerned. Some other physicochemical characteristics of this oil may influence the solubilization process.

We have previously reported [55] that AOT/IPM/water is nonpercolating and can be made percolating by the addition of nonionic(s) to this system. The percolation behavior of AOT/nonionic/IPM/water system is different from those of AOT/nonionic/hydrocarbon oil/water systems [55]. It has been reported that the process of coalescence of droplets followed by exchange of materials is accompanied by oil removal from the interface, and the interfacial fluidity may increase with increasing ease of oil removal [74]. The absorption of oil molecules into the interface increases significantly for oils with smaller chain length than that of the surfactant, which in turn hinders the droplet coalescence process. On the other hand, for oils with larger chain length (or higher molar volumes), penetration into the interface is reduced and

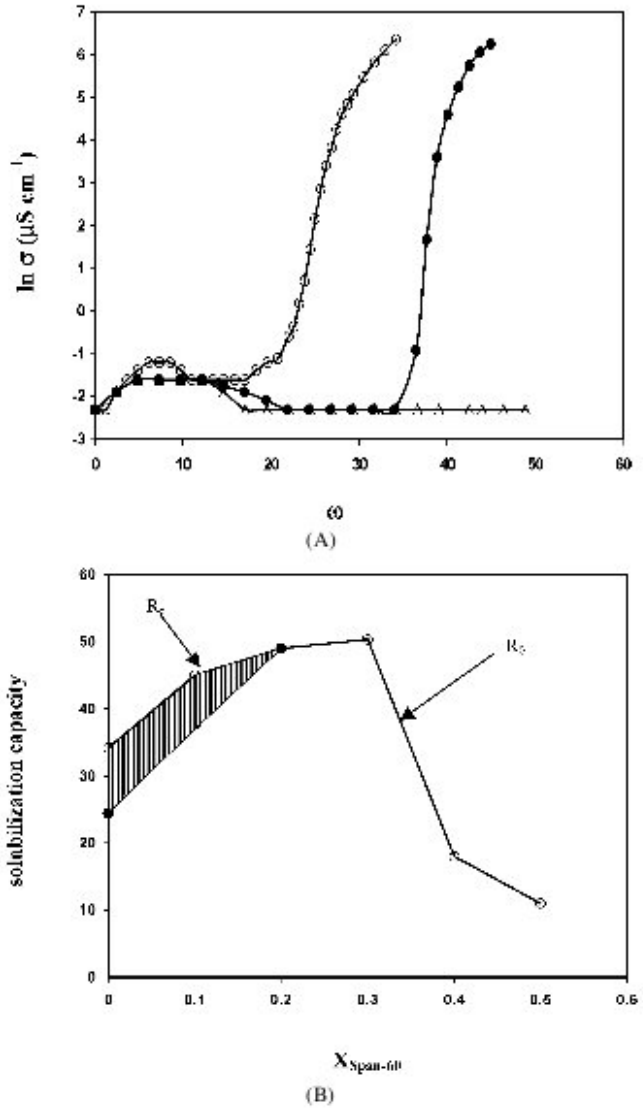

Fig. 9. Conductance study and percolation region of the system AOT/Span-60/Dc/water at 303 K with total surfactant concentration 0.25 mol dm^{-3}. (A) Span-60: (○) $X = 0$; (●) $X = 0.1$; (△) $X = 0.2$. (B) The shaded region represents the percolation region. R_0 indicates the curvature branch and R_c indicates the interdroplet interaction branch.

hence removal of oil molecules from the interface during collision is eased. So the percolation phenomenon is facilitated for hydrocarbon oils with higher molar volumes. In order to investigate the percolating nature of a mixed surfactant system stabilized in a hydrocarbon oil with higher molar volume (Dc) than that of Cy and IBB, we studied the conductance behavior of AOT/Span-60/Dc/water system which exhibited solubilization maximum in AOT/Span-60 blended system. The conductivity of this system at different $X_{\text{Span-60}}$ as a function of ω and the corresponding percolation region in the solubilization capacity vs X_{nonionic} profile are presented in Figs. 9A and 9B. It is interesting to note that AOT/Dc/water system has been found to be percolating, which indicates the strong attractive interaction between the droplets and the fluid nature of the interface [25–27]. Addition of Span-60 decreases the fluidity of the interface and the attractive interaction among the droplets, which results in a solubilization maximum. The result is also supported by the fact that ω_p increases for $X_{\text{Span-60}} = 0.1$ compared to $X_{\text{Span-60}} = 0$ and no percolation is observed for $X_{\text{Span-60}} = 0.2$. This observation confirms the discussion made in the previous section (3.2.3) that the long-chain hydrocarbon with higher molar volume (Dc) obeys the model proposed by Shah and co-workers [25–27], but this model fails to interpret the results for systems stabilized by a non-hydrocarbon type of oil, IPM. On the other hand, percolation behavior somewhat resembles that of oils of low molar volume (Cy and IBB). It can be noted that the chemical structure and polarity due to the presence of ester group of IPM differs from those of hydrocarbon oils. Hence it can be inferred from all these investigations that IPM may influence the molecular structure of the interface, which governs the solubilization behavior in reverse micellar systems, in a way different from that of the studied hydrocarbon oils [25,29,30,75]. The present paper is the first report of solubilization behavior in mixed reverse micellar systems using oils with different characteristics. Further study in this direction is needed. But the main focus must be on how the chemical structure of the oils alters the interfacial composition and its geometry in order to exhibit such behaviors.

3.4.2. NaCl (aq)/mixed surfactants/oil

Conductance studies are carried out for the systems AOT/nonionic(s)/IPM/aq. NaCl (of different concentrations including $[\text{NaCl}]_{\max}$) at 303 K at the corresponding $X_{\text{nonionic,max}}$. Brij-56, Brij-58, Span-20, and Span-80 are used as the nonionic(s) in these studies. Of these studies, the conductivity of AOT/Brij-56/IPM/aq. NaCl system at $X_{\text{Brij-56,max}} = 0.1$ as a function of [NaCl] and ω, and percolation zones in the solubilization capacity–[NaCl] profile of AOT/Brij-56 and Brij-58 systems are presented in Figs. 10A and 10B. It is found that percolation occurs at $[\text{NaCl}] < [\text{NaCl}]_{\max}$. As [NaCl] increases, the percolation threshold (ω_p) increases. On the other hand, it is also indicated that the presence of NaCl shifts the percolation threshold (ω_p) toward higher ω with respect to water at comparable composition. Similar results has been observed for DDAB/Brij-56/IPM/aq. NaBr at $X_{\text{Brij-56,max}} = 0.3$ (figure not shown).

It reveals from the dye solubilization study for the system AOT/Brij-56 or Brij-58/IPM/NaCl (aq) at $X_{\text{nonionic,max}}$ that the ascending curve is the interdroplet interaction branch (R_c) and the descending curve is the curvature branch (R_0) in the solubilization capacity vs [NaCl] profile. This observation is well supported from the conductivity measurements, wherein percolation of conductance has been exhibited by the samples chosen from the ascending curve (indicating droplets with fluid interfaces). On the other hand, the samples chosen from the descending branch have been found to be low-conducting and a noninteracting hard sphere type droplet structure can be assumed. It has been mentioned ear-

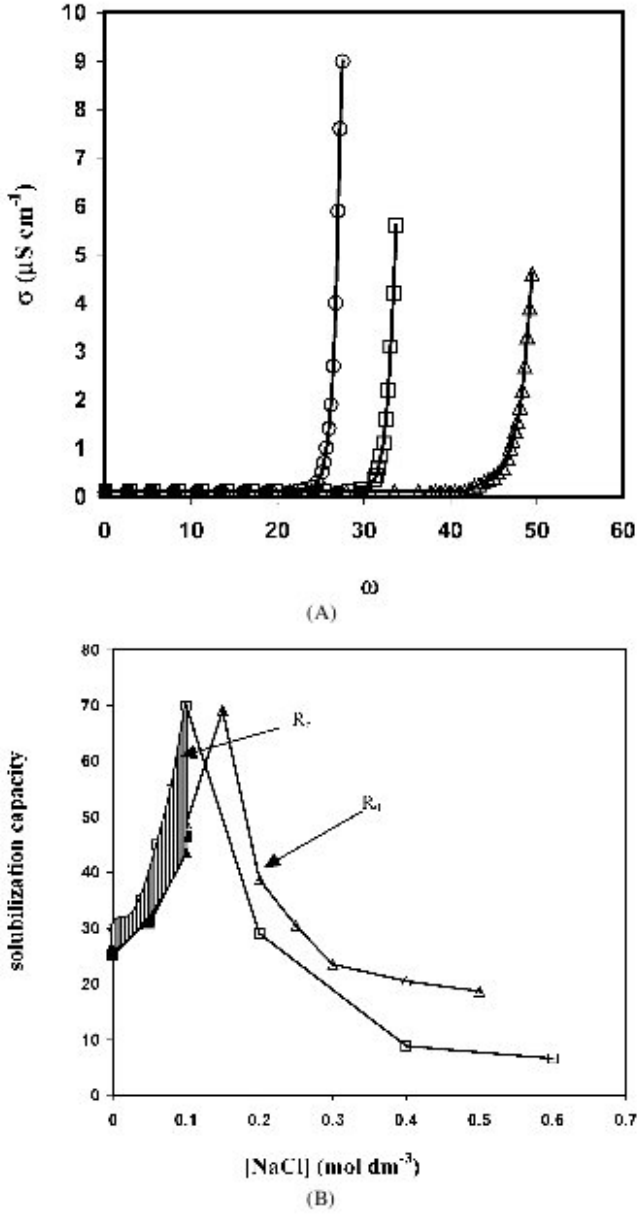

Fig. 10. Conductance study and percolation region of the system with total surfactant concentration 0.1 mol dm^{-3}. (A) AOT/Brij-56/IPM/NaCl at 303 K with $X_{\text{Brij-56}} = 0.1$. (○) water; (□) 0.05 mol dm^{-3} NaCl; (△) 0.1 mol dm^{-3} NaCl; (●) 0.15 mol dm^{-3} NaCl. (B) The shaded portion denotes the percolation region. (□) AOT/Brij-56; (△) AOT/Brij-58. R_0 indicates the curvature branch and R_c indicates the interdroplet interaction branch.

lier that the solubilization behavior of AOT/Brijs/IPM/water systems at $X_{\text{nonionic,max}}$ is governed by the interdroplet interaction and addition of electrolyte enhances the solubilization capacity. It can be argued that any factor that makes this interaction less feasible would increase the solubilization capacity. It is known that the addition of electrolyte diminishes the effective polar head area of the surfactants by screening the electrostatic repulsion, which makes surfactant membranes more rigid and decreases the attractive interactions among the droplets [25,27,28,46,76]. In presence of NaCl, large activation energies are needed to create positive curvature of local regions and thus percolation is hindered. This in turn increases the solubilization capacity. Thus ω_p for water (i.e., in the absence of NaCl) remains minimum and then increases with increase in [NaCl] (Fig. 10A). But at a certain NaCl concentration, $[\text{NaCl}]_{\max}$, the droplets become very rigid and starts behaving like hard sphere type, wherein no percolation has been observed and solubilization capacity decreases with increasing [NaCl]. Hence the descending curve can be attributed due to the curvature effect as evidenced from the conductivity measurements.

4. Conclusions

The addition of Brij-30, Brij-35, Brij-52, Brij-56, Brij-58, Brij-76, Tween-20, Tween-40, Span-20, Span-40, Span-60, Span-80, and Igepal CO 520 in AOT/IPM reverse micellar systems induces synergism in solubilization capacity of water. The addition of Brij-56, Brij-58 in DDAB/IPM, DDAB/Cy, and DDAB/IBB systems also induces synergism in water solubilization, whereas declining trend in solubilization is observed for Brij-56 in DDAB/IBB system. For AOT/Cy and AOT/IBB reverse micellar systems, the addition of Brij-35, Brij-56, Brij-58, Tween-20, and Tween-40 induces enhancement of water solubilization, whereas Brij-52 and Spans fail to do so. No synergism has been observed for Igepal CO 520 and Brijs, Spans blended systems in IPM, whereas the addition of Brij-56 and Brij-58 in Igepal CO 520 stabilized in Cy and IBB exhibits synergism.

The maximum in solubilization capacity of water ($\omega_{0,\max}$) occurs in most of these systems at a certain mole fraction of the nonionic surfactant, $X_{\text{nonionic,max}}$, depending upon EO chain and configuration of the polar head group and hydrocarbon moiety of the nonionic surfactants and on the type of oil.

The addition of electrolyte (NaCl or NaBr) enhances or diminishes the solubilization of water in these mixed reverse micellar systems depending upon the composition of the nonionic surfactant (X_{nonionic}) used. Solubilization capacity is further enhanced, and maximum in solubilization ($\omega_{\max}$) is obtained at an optimum electrolyte concentration ($[\text{NaCl}]_{\max}$ or $[\text{NaBr}]_{\max}$) for mixed surfactant systems at the respective $X_{\text{nonionic,max}}$ and also at $X_{\text{nonionic}} = 0.1$. The extent of this enhancement in $\omega_{\max}$ depends on content, EO chains and configuration of polar head group of nonionic surfactants, as well as on the concentration of NaCl. It has been found that $[\text{NaCl}]_{\max}$ is higher for the nonionic surfactants with larger polar head group. The oils play a significant role in the solubilization of water and aqueous NaCl in the mixed systems due to their difference in chemical structure and physical properties.

The maximum in solubilization in mixed reverse micelles stabilized in Cy, IBB and Dc oils can be interpreted with the help of the model developed by Shah and co-workers

[23–25], but it fails to account for the same observed for mixed blended systems stabilized in IPM oil.

No percolation in conductance can be observed for AOT-stabilized systems in IPM and IBB. ω-induced percolation in conductance is obtained for AOT/nonionics/IPM/water and AOT/nonionics/IBB/water reverse micellar systems at $X_{\text{nonionic}} \geqslant X_{\text{nonionic,max}}$, which indicates that the ascending curve in the solubilization capacity–X_{nonionic} profile as the curvature branch due to the rigidity of the interface (R_0) and the descending curve is the interdroplet interaction branch (R_c) in these mixed systems. On the other hand, AOT/Span-60/Dc systems percolate with $X_{\text{nonionic}} \leqslant X_{\text{nonionic,max}}$. The results obtained with IBB and Dc oils fit well with the Shah model, whereas those obtained with IPM oil do not fit with the model.

No percolation is observed for both AOT and AOT/nonionics stabilized in Cy.

Both AOT and DDAB blended systems stabilized in IPM and electrolyte exhibit percolation at $X_{\text{nonionic,max}}$ at [electrolyte] $\leqslant$ [electrolyte]$_{\max}$, wherein reversal of the curvature branch (R_0) and interdroplet interaction branch (R_c) with respect to the aqueous systems in solubilization capacity–[electrolyte] profile is observed.

Appearance of solubilization maxima in these mixed surfactant systems (in absence and presence of electrolytes) can be correlated with the occurrence of percolation of conductance in such systems.

Acknowledgments

The authority of Indian Statistical Institute, Kolkata, is acknowledged for financial support in the form of a Project and a Senior Research Fellowship to R.K.M.

Supplementary material

The online version of this article contains additional supplementary material. Please visit DOI: 10.1016/j.jcis.2005.02.088.

References

[1] T.K. De, A.N. Maitra, Adv. Colloid Interface Sci. 59 (1995) 95, and references therein.
[2] K. Kon-No, Surf. Colloid Sci. 15 (1993) 125.
[3] C. Solans, H. Kunieda, Industrial Application of Microemulsions, Dekker, New York, 1997.
[4] J. Sjoblom, R. Lindberg, S.E. Friberg, Adv. Colloid Interface Sci. 95 (1996) 125.
[5] S.P. Moulik, B.K. Paul, Adv. Colloid Interface Sci. 78 (1998) 99.
[6] P. Kumar, K.L. Mittal, Handbook of Microemulsions: Science and Technology, Dekker, New York, 1999.
[7] B.K. Paul, S.P. Moulik, J. Dispers. Sci. Technol. 18 (1997) 30.
[8] B.K. Paul, S.P. Moulik, Curr. Sci. 80 (2001) 990.
[9] N.L. Klyachko, A.V. Levashov, Curr. Opin. Colloid Interface Sci. 8 (2003) 179.
[10] P.L. Luisi, B.E. Straub (Eds.), Reverse Micelles: Biological and Technological Relevance of Amphiphilic Structures in Apolar Media, Plenum, New York, 1984.
[11] P.L. Luisi, L.J. Magid, CRC Crit. Rev. Biochem. 20 (1986) 409.
[12] E.B. Leodidis, T.A. Hatton, in: M.P. Pileni (Ed.), Structure and Reactivity in Reverse Micelles, Elsevier, Amsterdam, 1987, p. 270.
[13] A. Gupte, R. Nagarajan, A. Kilara, in: G. Charalambous (Ed.), Food Flavors: Generation, Analysis and Process Influence, Elsevier, Amsterdam, 1995.
[14] A. Goto, Y. Ibuki, R. Goto, in: A.G. Volkov (Ed.), Interfacial Catalysis, Dekker, New York, 2002, p. 391.
[15] T. Zemb, F. Tanford, in: K. Holmberg (Ed.), Solubilization, Handbook of Applied Surface and Colloid Chemistry, vol. 2, Wiley, New York, 2001, p. 159.
[16] K. Kon-No, A. Kitahara, J. Colloid Interface Sci. 41 (1972) 47.
[17] H.R. Rabie, D. Helou, M.E. Weber, J.H. Vera, J. Colloid Interface Sci. 189 (1997) 208.
[18] K. Kon-No, A. Kitahara, J. Colloid Interface Sci. 33 (1970) 124.
[19] K. Kon-No, A. Kitahara, J. Colloid Interface Sci. 34 (1970) 221.
[20] K. Kon-No, A. Kitahara, J. Colloid Interface Sci. 37 (1971) 469.
[21] T. Kawai, K. Hamada, N. Shindo, K. Kon-No, Bull. Chem. Soc. Jpn. 65 (1992) 2715.
[22] T. Kawai, K. Hamada, N. Shindo, K. Kon-No, Bull. Chem. Soc. Jpn. 66 (1993) 2802.
[23] K. Hamada, T. Ikedu, T. Kawai, K. Kon-No, J. Colloid Interface Sci. 223 (2001) 166.
[24] V.K. Bansal, D.O. Shah, J.P. O'Connell, J. Colloid Interface Sci. 75 (1980) 462.
[25] M.J. Hou, D.O. Shah, Langmuir 3 (1987) 1086.
[26] R. Leung, D.O. Shah, J. Colloid Interface Sci. 120 (1987) 320.
[27] R. Leung, D.O. Shah, J. Colloid Interface Sci. 120 (1987) 330.
[28] M.J. Hou, M. Kim, D.O. Shah, J. Colloid Interface Sci. 123 (1988) 398.
[29] A. Zada, J. Lang, R. Zana, J. Phys. Chem. 94 (1990) 381.
[30] R.E. Verrall, S. Milioto, R. Zana, J. Phys. Chem. 92 (1988) 3939.
[31] A. Derouiche, C. Tondre, J. Dispers. Sci. Technol. 12 (1991) 517.
[32] C. Caillet, M. Hebrant, C. Tondre, Langmuir 14 (1998) 4378.
[33] E.A. Abuin, M.A. Rubio, E.A. Lissi, J. Colloid Interface Sci. 158 (1993) 129.
[34] S.J. Chen, D.F. Evans, B.W. Ninham, J. Phys. Chem. 88 (1984) 1631.
[35] D.F. Evans, D.J. Mitchell, B.W. Ninham, J. Phys. Chem. 90 (1986) 2817.
[36] M. Olla, M. Monduzzi, L. Ambrosone, Colloids Surf. A 160 (1999) 23.
[37] M. Olla, M. Monduzzi, Langmuir 16 (2000) 6141.
[38] H. Mays, J. Pochert, G. Ilgenfritz, Langmuir 11 (1995) 4347.
[39] L. Schlich, J.H. Spilgies, F. Runge, S. Lipgens, S. Boye, D. Schübel, G. Ilgenfritz, Biophys. Chem. 58 (1996) 39.
[40] K.A. Johnson, D.O. Shah, J. Colloid Interface Sci. 107 (1985) 269.
[41] K.A. Johnson, D.O. Shah, in: K.L. Mittal, P. Bothorel (Eds.), Surfactants in Solution, vol. 6, Plenum, New York, 1986.
[42] P.D.I. Huibers, D.O. Shah, Langmuir 13 (1997) 5762.
[43] G. Ludensten, S. Backlund, G. Kiwilsza, Prog. Colloid Polym. Sci. 97 (1995) 194.
[44] N. Seedher, N. Manik, J. Surf. Sci. Technol. 9 (1993) 81.
[45] D. Liu, J. Ma, H. Cheng, Z. Zhao, Colloids Surf. A 143 (1998) 59.
[46] Q. Li, T. Li, J. Wu, Colloids Surf. A 197 (2002) 101.
[47] A. Bumajdad, J. Eastoe, P. Griffiths, D.C. Steytter, R.K. Heenan, J.R. Lu, P. Timmins, Langmuir 15 (1999) 5271.
[48] A. Bumajdad, J. Eastoe, Phys. Chem. Chem. Phys. 6 (2004) 1597.
[49] C. von Corswant, O. Soderman, Langmuir 14 (1998) 3506.
[50] A. Acharya, S.K. Sanyal, S.P. Moulik, Curr. Sci. 81 (2001) 362.
[51] A. Attwood, in: J. Kreuter (Ed.), Colloid Drug Delivery System, Dekker, New York, 1994, p. 31.
[52] R.K. Mitra, B.K. Paul, J. Surf. Sci. Technol. 19 (2003) 139.

[53] R.K. Mitra, B.K. Paul, J. Surf. Sci. Technol. 20 (2004) 105.
[54] R.K. Mitra, B.K. Paul, J. Colloid Interface Sci. 283 (2005) 565.
[55] R.K. Mitra, B.K. Paul, Colloids Surf. A 252 (2005) 243.
[56] R.K. Mitra, B.K. Paul, Colloids Surf. A 255 (2005) 165.
[57] A. Maitra, G. Vasta, H.F. Eicke, J. Colloid Interface Sci. 93 (1983) 383.
[58] D.M. Zhu, Z.A. Schelly, Langmuir 8 (1992) 48.
[59] K. Shinoda, H. Saito, J. Colloid Interface Sci. 8 (1992) 48.
[60] S.E. Friberg, in: H.F. Eicke, G.D. Parfitt (Eds.), Interfacial Phenomena in Apolar Media, Dekker, New York, 1987.
[61] F.O. Opawale, D.J. Burgess, J. Colloid Interface Sci. 197 (1998) 142.
[62] D.J. Mitchell, B.W. Ninham, J. Chem. Soc. Faraday Trans. II 77 (1981) 601.
[63] J.N. Israelachvili, B.W. Ninham, J. Chem. Soc. Faraday Trans. II 72 (1976) 1525.
[64] L.M.M. Nazario, T.A. Hatton, J.P.S.G. Crespo, Langmuir 12 (1996) 6326.
[65] S. Brunetti, D. Roux, A.M. Bollocq, J. Phys. Chem. 87 (1983) 1028.
[66] D. Roux, A.M. Bellocq, P. Bothorel, in: K.L. Mittal, B. Lindman (Eds.), Surfactants in Solution, Plenum, New York, 1984, p. 1843.
[67] F. Akoum, O. Parodi, J. Phys. 46 (1981) 1675.
[68] E.B. Leodidis, T.A. Hatton, Langmuir 5 (1989) 741.
[69] S.P. Moulik, B.K. Paul, in: J.A. Schwarz, C.I. Contescu (Eds.), Surfaces of Nanoparticles and Porous Materials, Dekker, New York, 1999, chap. 11.
[70] D. Liu, J. Ma, H. Cheng, Z. Zhao, Colloids Surf. A 135 (1998) 157.
[71] D. Liu, J. Ma, H. Cheng, Z. Zhao, Colloids Surf. A 148 (1999) 291.
[72] H. Mays, J. Phys. Chem. B 101 (1997) 10271.
[73] D. Liu, J. Ma, H. Cheng, Z. Zhao, J. Dispers. Sci. Technol. 20 (1999) 513.
[74] B. Lemaire, P. Bothorel, D. Roux, J. Phys. Chem. 87 (1983) 1023.
[75] J. Lang, R. Zana, N. Lalem, in: D.M. Bloor, E. Wyn-Jones (Eds.), The Structure, Dynamics and Equilibrium Properties of Colloidal Systems, Kluwer Academic, Dordrecht, 1990, p. 253.
[76] B. Bedwell, E. Gulari, J. Colloid Interface Sci. 102 (1984) 88.